Two-way coupled particle-turbulence interaction: Effect of numerics and resolution on fluid and particle statistics

J. A. K. Horwitz[1,2,*] and A. Mani[2]
[1]*Lawrence Livermore National Laboratory, P.O. Box 808, Livermore, California 94550-0808, USA*
[2]*Department of Mechanical Engineering, Stanford University, Stanford, California 94305, USA*

(Received 27 September 2019; accepted 28 August 2020; published 12 October 2020)

Euler-Lagrange point-particle simulation has emerged as a premier methodology for studying dispersed particle-laden flows. This method's popularity stems from its ability to resolve fine-scale fluid structures while also tracking individual particles at reduced cost using an appropriate particle acceleration model. However, the point-particle model has known convergence issues in that refinement of the fluid grid can lead to changes in the predicted statistics. The reasons for nonconvergence are twofold: the point-particle two-way coupling force in the Navier-Stokes equations requires a numerical regularization and, without careful implementation, yields a singular force on the fluid with grid refinement. The second factor that yields grid-dependent statistics is that the point-particle force model in general depends on the undisturbed fluid velocity. When the undisturbed fluid velocity is not robustly modeled in a grid-insensitive way, the calculated force for both particles and fluid will be grid-dependent, contaminating their respective statistics. While the first issue regarding regularizing the point-particle source term has received attention in the literature, the consequences of robustly modeling the undisturbed velocity in the context of grid refinement of turbulence has received little attention. In this work, we consider decaying homogeneous isotropic turbulence laden with particles at different Stokes numbers. For a given Stokes number, we systematically refine the grid and demonstrate that explicitly modeling the undisturbed fluid velocity yields relative grid insensitivity for the energy of the particle and fluid phases, as well as acceleration of the particles. We also demonstrate that an appropriately defined dissipation rate is also grid-insensitive when an undisturbed fluid velocity correction is used. In contrast, when the undisturbed fluid velocity is modeled using the conventional approach of interpolating the local fluid velocity to the particle location, we show this procedure yields divergent statistics with grid refinement. In particular, we show that higher-order interpolation of the fluid velocity in two-way coupled problems is worse than lower-order interpolation, in the absence of a correction procedure to estimate the undisturbed fluid velocity. We also examine velocity derivative statistics of the fluid phase and demonstrate that these statistics are not in general convergent even when the undisturbed fluid velocity is explicitly modeled. Collectively, the observations in this work are used to present a philosophy on the types of questions which are answerable with point-particle methods.

DOI: 10.1103/PhysRevFluids.5.104302

*Corresponding author: horwitz3@llnl.gov

I. INTRODUCTION

In the decades since the term "point particle" was used by Saffman in 1973 [1], it has become a leading paradigm for the numerical simulation of coupled particle-laden flows. The term is not unfamiliar to other branches of physics to describe, for example, small charged particles like electrons. Conceptually, the point-particle idea represents a model reduction whereby physical phenomena near small particles are modeled instead of resolved. To understand what effects may need to be modeled, it is important to first develop the view of physical description resulting from sufficient resolution.

In the context of fluid suspensions where small solid particles interact hydrodynamically, the governing equations describing the system are well known. Fluid and solid material evolve owing to their respective momentum equations, and the fluid momentum equation is called the Navier-Stokes equation for Newtonian fluids following Batchelor's notation [2]. At the boundary of the dispersed and continuous phase, physical boundary conditions close the problem. For many applications, the no-slip and no-penetration boundary conditions accurately describe the behavior of fluid elements in the neighborhood of dispersed phase boundaries. The condition of local dynamic equilibrium at particle boundaries, namely, that fluid and solid are not in relative motion, does not in general imply that the respective phases are globally in dynamic equilibrium. The presence of fluid viscosity allows for a deviatoric stress distribution to exist in the fluid which cannot preclude the deformation of fluid elements. Therefore in viscous fluids, the condition of dynamic equilibrium at phase boundaries generally accompanies stress nonequilibrium. The integrated stress over the particle surface will in general result in a change of both its linear and angular momentum.

The above picture is how we view reality, how we would describe particle-fluid interactions in an experiment, and how we would set up a numerical calculation given the available resources. The latter example is what has come to be called Particle Resolved Direct Numerical Simulation (PR-DNS). In PR-DNS, the Navier-Stokes equations are solved on a fine enough grid to resolve all fluid scales including the boundary layer between each particle and the fluid. This allows the fluid stress distribution to be calculated on the scale of the particle. The net force and torque experienced by each particle then causes them to translate and rotate [3]. PR-DNS, while a powerful tool, often contains some model simplifications. In many gas-solid flows, the stress distribution is not solved for directly inside particles. During collisions, spring-mass-damper models are often used [4]. PR-DNS has only recently become possible owing to the computational resources it requires with grid resolution depending on volume fraction and Reynolds number [5,6], and some recent studies include [5–11]. The point-particle method on the other hand uses a coarser grid, one which cannot resolve all fluid scales (including the ones created by the particle phase) [12–15]. Historically, the community has divided point-particle methods into two categories, point-particle DNS (PP-DNS) and point-particle LES (PP-LES). In PP-DNS, the fluid grid is chosen to resolve all fluid scales in the absence of the particle phase, whereas in PP-LES, the grid is coarser than PP-DNS. In both PP-DNS and PP-LES, the fluid phase has unresolved scales. The former has unresolved scales exclusively owing to the dispersed phase, and the latter has unresolved scales owing to the dispersed phase and unresolved small scales that would exist even in absence of the dispersed phase. While PP-LES has met some success in reproducing PP-DNS isotropic turbulent predictions [16], challenges in predicting turbulence modification in turbulent channel flow [17] has been a motivation for development of more sophisticated point-particle methods applicable to both PP-LES and PP-DNS [18–20].

The unresolved scales owing to the particle phase are a characteristic of the point-particle method. Because the fluid grid in PP-DNS and PP-LES is not fine enough to resolve the stress distribution at the particle scale, a model must instead be used to couple the particle and fluid phase. This model is called the point-particle method. In the point-particle method, models for the integrated stress are prescribed which allow the force (and less commonly) the torque to be calculated from computed (resolved) quantities. These models are chosen by the assessing the nondimensional parameters of a given problem. For example, if one wishes to simulate a single

particle moving unidirectionally at low Reynolds number in an unbounded domain, it is known that the particle obeys Stokes drag [21] and experiences no lift or torque. Since this particle is experiencing a net force, Newton's second law says the particle will experience a rate of change of its linear momentum. Two integrations respectively give a new velocity and position for the particle.

How is the point-particle's motion coupled to the fluid? In the PR-DNS method, the particle location and velocity provide a boundary condition to the fluid. In PP-DNS and PP-LES, no boundary condition is imposed. Rather, as was suggested by Saffman [1], the particle is represented by a multipole expansion, where the force and torque represent the coefficients in the multipole expansion. For a nonrotating particle moving under Stokesian conditions, we have just the force term. Using observed quantities, the drag force may be calculated, but since the particles may exist anywhere in space while fluid quantities are generally stored at fixed Eulerian locations, the calculated drag force must be projected back to the fluid grid. This drag force serves to slow down the fluid local to the particle. Suppose we seek to calculate the drag force at the next time step. The fluid velocity near the particle will now have two components, one which is just due to the underlying flow field, and the second, which is owing to a disturbance field created by that particle. To calculate the new drag force there is now a problem, because drag laws, whether they be Stokes drag [21] or a more complicated formula, are formulated *a priori*, that is, they are formulated based on "undisturbed" variables evaluated at the location of the particle. For example, $F_{\text{Stokes}} = 3\pi\mu d_p(\tilde{u}_p - v_p)$. The drag the particle experiences which is equal to and opposite to the force exerted on the fluid is proportional to the fluid viscosity μ, the particle diameter d_p, and the difference between the undisturbed fluid velocity evaluated at the particle location, $\tilde{u}_p$, and the particle velocity, v_p. The undisturbed fluid velocity $\tilde{u}_p$ found in every known drag law is not trivial to evaluate in two-way coupled point-particle simulations precisely because the fluid velocity which could be naturally computed at the location of the particle by interpolating from surrounding fluid grid points will contain an additional disturbance velocity created by that particle.

In a recent paper [22], we proposed a correction method to estimate the undisturbed fluid velocity from the computed velocity field which contained a velocity disturbance generated by a point particle. The correction was formulated by recognizing that the disturbance field created by a point particle is nearly symmetric in the Stokes limit and locally looks like an enhanced curvature in the fluid velocity field. We presented a verification problem involving a settling particle in an otherwise quiescent flow and found that the proposed correction was able to reproduce the analytical settling velocity for a range of parameters. We also showed that if this correction is not accounted for, the drag force a particle experiences will be underpredicted, which results in an artificially higher settling velocity. We showed this error increases for two reasons: as the particle to grid size increases, so too does the computed disturbance field. This means the fluid velocity near the particle is farther from the undisturbed value. In other words, as a particle moves and drags fluid with it, a slip velocity calculated using the difference between the disturbed and particle velocity will always be lower than the slip velocity calculated using the difference between the undisturbed fluid and particle velocity. The second error comes from the choice of interpolation scheme. Higher order interpolation schemes used to calculate the (disturbed) fluid velocity at the location of the particle resulted in larger errors in settling velocity compared with lower-order schemes. This was explained by the fact that higher-order schemes provide a better estimate of the computed disturbed fluid velocity at the location of the particle, which is farther from the correct value of the undisturbed fluid velocity which is sought for in the drag formula. Hence, a new paradigm has arisen in the simulation of two-way coupled flows with point particles: *in the absence of using a scheme to correct for the undisturbed fluid velocity, lower-order interpolation schemes should be used.*

The above observation was counter to standard practice, namely using higher-order interpolation projection for Lagrangian-Eulerian data transfer, which had been the standard paradigm since the seminal work of Sundaram and Collins [23], owing to symmetries in the quadratic form for point-particle dissipation. In the limit of very small particles compared to the grid size, the Sundaram and Collins derivation was exact. However, it was shown in [6] that explicitly accounting for the undisturbed fluid velocity (which may differ greatly from the interpolated fluid velocity at the

particle location when $d_p \ll dx$) causes the symmetry in the quadratic form to disappear. In that work, it was argued that in two-way coupled point-particle simulation, regardless of what projection scheme is used, it is best to calculate the drag force as accurately as possible by explicitly modeling the undisturbed fluid velocity. Together Refs. [6,22] showed, under homogeneous conditions, that *a consequence of explicitly modeling the undisturbed fluid velocity was that the implied dissipation rate, defined as the resolved plus the point-particle model form dissipation rate together would equal the analytically correct dissipation rate consistent with the prescribed drag force.* In this work, we will refer to this observation as the *correspondence principle*. In recent years, several methods have been proposed for estimating the undisturbed fluid velocity [15,18,24–26]. The details of each of these methods will be briefly discussed in the methods section. Overall, the goal of the present study is understanding what are the consequences of explicitly modeling the undisturbed fluid velocity in two-way coupled particle-laden turbulence versus not modeling the undisturbed fluid velocity. In this work, we will use the approach developed in Horwitz and Mani [22].

The purpose of this paper may now be addressed. Having developed a verifiable method for computing Stokes drag in two-way coupled flows, the aim of this paper is to examine the effect of computing Stokes drag with and without this correction in a more complicated flow environment. In this work, using PP-DNS, we will examine decaying homogeneous isotropic turbulence laden with small inertial particles of different Stokes numbers. The problem we wish to answer is, in an otherwise dynamically equivalent setup, e.g., fixed mass loading, particle size, Stokes number, initial Reynolds number, etc., how do fluid and particle statistics change if we model the coupling between fluid and particles as Stokes drag, and calculate the fluid velocity, on the one hand using the undisturbed fluid velocity, and on the other hand, using the disturbed fluid velocity, calculating the latter quantity with standard interpolation schemes? For the dynamically equivalent setup, how do the statistics change as the fluid grid is refined? In Sec. II we summarize the PP-DNS algorithm including the different formulations for computing the particle drag force. In Sec. III the results of the simulations are presented and discussed. Concluding remarks are given in the final section.

II. METHODS

We are using the code originally developed by Pouransari [27]. We use an Eulerian-Lagrangian formulation which solves the Navier-Stokes equations (1) subject to the constraint of continuity (2):

$$\frac{\partial}{\partial t}\rho_f u_i + \frac{\partial}{\partial x_j}\rho_f u_i u_j = -\frac{\partial p}{\partial x_i} + \mu\frac{\partial^2 u_i}{\partial x_j \partial x_j} - \sum_k^{N_p} F_i^k P\{\delta(\mathbf{x}-\mathbf{x}^k)\}, \tag{1}$$

$$\frac{\partial}{\partial t}\rho_f + \frac{\partial}{\partial x_j}\rho_f u_j = 0. \tag{2}$$

Here, ρ_f and μ are, respectively, the fluid density and dynamic viscosity, u_i and p are respectively the fluid velocity and pressure, and F_i^k is the drag force on the kth particle. The summation is over the total number of particles N_p in a control volume, and P is a projection operator, to be defined, which is used to transfer discrete Lagrangian data to the Eulerian mesh. The fluid solver is a second-order finite difference-based scheme. Time integration of fluid and particle equations is performed using explicit fourth-order Runge-Kutta. A divergence-free velocity field is enforced via a Poisson equation for pressure; the pressure equation is solved directly using fast Fourier transforms. The kth particle is tracked in a Lagrangian frame. The position and velocity of each particle are updated using (3) and (4), respectively:

$$\frac{dx_i^k}{dt} = v_i^k, \tag{3}$$

$$m_p\frac{dv_i^k}{dt} = F_i^k = \frac{m_p}{\tau_p}\left(\tilde{u}_i^k - v_i^k\right). \tag{4}$$

Here, x_i^k and v_i^k are, respectively, the position and velocity of the kth particle, $\tau_p = \rho_p d_p^2/18\mu$ is the particle relaxation time, where ρ_p and d_p are, respectively, the particle density and diameter. The mass of the particle, m_p, is $(\pi/6)\rho_p d_p^3$. The drag force F_i^k of the kth is assumed to be Stokesian. In Stokes's formula, the undisturbed fluid velocity at the location of the particle is $\tilde{u}_i^k$. In the discussion to follow, when we speak of calculating the disturbed fluid velocity, it means Eq. (4) is being used with u_i^k, that is, the fluid velocity from the surrounding grid points interpolated to the particle position. The distinction between the undisturbed and disturbed fluid velocity pertains only to the two-way coupled problem, which is the focus of this paper.

To complete the Euler-Lagrange algorithm we must specify the method for calculating the fluid velocity used in Stokes's formula and the projection operator in (1). In this work, we consider two paradigms for calculating the velocity that appears in Stokes drag. The first paradigm is an explicit model for the undisturbed fluid velocity at the particle location. The explicit model we use in this work was developed in [22]. In that work, we proposed estimating the undisturbed fluid velocity via a formula of the form

$$\tilde{u}_i^k\left(x_i^k(t)\right) = u_i^k\left(x_i^k(t)\right) + C^k\left(\Lambda, x_i^k(t)\right)\nabla^2 u_i^k\left(x_i^k(t)\right). \tag{5}$$

Conceptually, Eq. (5) suggests that the undisturbed fluid velocity at the particle location, $\tilde{u}_i^k(x_i^k(t))$, differs from the fluid velocity which could be naturally interpolated to the particle location, $u_i^k(x_i^k(t))$, because this latter fluid velocity contains a component owing to the fluid disturbance created by the particle force. This model assumes the additional disturbance velocity correlates to enhanced curvature in the fluid velocity field in the neighborhood of the particle. The correction scheme depends on an empirical coefficient $C^k(\Lambda, x_i^k(t))$ which has been calibrated for different ratios of the particle to grid size $\Lambda = d_p/dx$ and depends on the location of the particle within a grid cell. In other words, for a computational user incorporating particles of a known size and a fluid grid with a known grid spacing, we have tabulated the amount of correction required in the form of $C(\Lambda)$. This calibration for different nondimensional particle sizes was an effort to remove grid sensitivity from the point-particle algorithm. Relative grid insensitivity has been demonstrated for the corrected point-particle algorithm under laminar conditions [22]. It is important to note that these C coefficients were developed specifically for spherical particles and the second-order finite difference solver used in this work. Different coefficients may be required for other spatial discretizations [20]. In this work, it will be important to test whether the corrected point-particle algorithm is relatively grid-insensitive under turbulent conditions. To compute the undisturbed fluid velocity at the particle location, the disturbed fluid velocity $u_i^k(x_i^k(t))$, the correction coefficient, $C^k(\Lambda, x_i^k(t))$, and disturbed fluid velocity Laplacian, $\nabla^2 u_i^k(x_i^k(t))$ are trilinearly interpolated to the particle location at each sub-step of the Runga-Kutta solver. Though this method of estimating the undisturbed fluid velocity was developed under laminar conditions, scaling analysis [6,26] has demonstrated this scheme is applicable in turbulent environments provided the particle size is small compared to the Taylor microscale. Incorporation of this correction procedure to estimate the undisturbed fluid velocity combined with a suitable drag law for particles has shown good agreement when compared to fully resolved Kolmogorov-sized particles [6].

There are other methods which have been developed to explicitly estimate the undisturbed fluid velocity for particle-laden flows. Recent works [15,24,25] have been developed whereby the projection operator in Eq. (1) is assumed Gaussian. The method of Gualtieri *et al.* [24] characterizes some of the unsteadiness in the particle drag force by transiently releasing vorticity into the fluid once the particle disturbance can be resolved on the grid. The work of Ireland and Desjardins [25] and Balachandar *et al.* [15] are based on analytical solutions to the Stokes equations assuming a Gaussian-regularized point force. In addition, Balachandar *et al.* has extended their analysis to the Oseen equations to account for finite Reynolds number effects on drag. They also develop analytical results for other undisturbed quantities appearing in the Maxey-Riley-Gatignol equation [28,29]. Esmaily and Horwitz [18] have also developed a scheme to estimate the undisturbed fluid velocity by appealing to solid mechanics and determining the drag force required to move

a control volume at its average velocity. All of these works have examined the accuracy of an undisturbed velocity correction under laminar conditions and compare favorably with [22]. The works [6,18,25,26] have demonstrated that incorporation of an undisturbed fluid velocity correction can have a significant effect on particle and/or fluid statistics in a turbulent environment. However, to the best of our knowledge, there has not been a point-particle study examining the effect of an undisturbed fluid velocity correction applied in the two-way coupling regime (significant mass loading) under turbulent conditions while also exploring the effect of grid refinement. In this work, we employ the scheme developed in [22] to estimate the undisturbed fluid velocity. In the Discussion section, we will mention where we expect other correction schemes to produce similar behavior and where we expect the results of our method to differ from other methods, had the latter been used to study the model problems presented here.

There is a second paradigm for treating the fluid velocity appearing in Stokes's formula, namely, to make no make no explicit model of the undisturbed fluid velocity and simply interpolate the (disturbed) fluid velocity from the surrounding fluid grid points. In [22,30], we showed under laminar conditions that higher-order interpolation of the disturbed fluid velocity would result in larger error. The reason this happens is because a better estimate of the disturbed fluid velocity translates to a worse estimate of the undisturbed fluid velocity. Therefore, in this work, it will be worth testing whether the observations about order of accuracy of interpolation of the disturbed fluid velocity hold under turbulent conditions. In this work we will consider trilinear, fourth-order Lagrange (Lagrange-4), and Cubic-Spline interpolation schemes.

To complete the point-particle algorithm, the projection operator should be defined. The correction procedure [22] adopted in this work is consistent with trilinear projection. In comparing the results for the undisturbed fluid velocity correction to those obtained with a disturbed fluid velocity, we use a symmetric projection operator for the latter results. In other words, trilinear interpolation of the fluid velocity will be combined with trilinear projection of the drag force, Lagrange-4 interpolation with Lagrange-4 projection, and Spline interpolation combined with Spline projection. This method was chosen to be consistent with the recommendation of [23] who suggested that the point-particle dissipation term would be consistent if symmetric interpolation-projection was used. However, we recall that work did not account for the difference between the undisturbed and disturbed fluid velocity; doing so removes the symmetry in the quadratic form [6], central to the arguments of [23]. While their derivation [23] is asymptotically correct when $\Lambda \rightarrow 0$, the dissipation error may be large (as we will show in the Results section) for finite Λ. Notwithstanding, symmetric interpolation projection as well as nonsymmetric direct interpolation of disturbed fluid velocity/particle drag force has been the leading paradigm for point-particle simulations for the last few decades, with a number of studies incorporating these paradigms within the past year, e.g., [31–37]. Therefore, it will be important to test this traditional paradigm in turbulent settings subject to grid refinement.

III. RESULTS AND DISCUSSION

The model problem we investigate in this work is decaying particle-laden isotropic turbulence. This model problem was chosen to understand how particles modify turbulence under homogeneous conditions [12,38,39]. Previously, we explored the effect of our correction scheme in a forced low mass loading suspension and observed that slip velocity statistics of particles showed less sensitivity to grid refinement when the undisturbed velocity is modeled compared with when the fluid velocity is the interpolated disturbed fluid velocity [26]. Studying a decaying turbulent suspension will allow us to examine turbulence modification without the difficulty in interpreting how the particle two-way coupling term is influencing a stationary forcing term in the Navier-Stokes equations. As we will show in the results section, a suitable normalization of the statistics will demonstrate that a decaying suspension is a viable setting to study turbulence modification under grid refinement.

The paradigm used to study the model problem is point-particle "direct" numerical simulation (DNS). The term "DNS" here is understood to mean that the Kolmogorov scale is resolved [40],

TABLE I. Summary of parameters used in decaying particle-laden cases.

N^3	$224^3,\ 448^3,\ 896^3$
$k_{\max}\eta_0$	3.14, 6.28, 12.57
$k_{f,0}$	0.01309, 0.01309, 0.01309
$\varepsilon_{f,0}$	0.001549, 0.001598, 0.001611
$\mathrm{Re}_{\lambda,0}$	27.2, 26.7, 26.6
T_e	8.45, 8.19, 8.13
Δt	0.015, 0.0075, 0.00375
η_0	0.028
L	2π
ν	0.001
Λ	0.25, 0.5, 1.0
$\mathrm{St}_{\eta,0}$	3.5, 10, 100
ρ_p/ρ_f	1008, 2880, 28 800
N_p	$1.36\times10^6,\ 4.77\times10^5,\ 4.77\times10^4$
ϕ	$9.92\times10^{-4},\ 3.47\times10^{-4},\ 3.47\times10^{-5}$
d_p	0.007012
d_p/η_0	0.25
ϕ_m	1.0

without consideration of the fluid scales introduced by the particle phase. In the results section, we will demonstrate that some fluid and particle statistics are grid-insensitive when the undisturbed fluid velocity is accounted for while some statistics are not in general grid convergent. This will help clarify how a point-particle "DNS" compares and differs from a traditional direct simulation of single phase flow.

The simulations in this work are summarized in Table I. The simulations are initialized with a divergence-free velocity field in a periodic box using Rogallo's procedure [41]. The initial velocity field obeys Pope's model spectrum [40]. Three grid resolutions $N^3 \in [224^3, 448^3, 896^3]$ are considered in this study. The number of grid points required for the finer simulations dictated a relatively low initial Taylor Reynolds number, $\mathrm{Re}_{\lambda,0} \approx 27$. The turbulence develops from the initial condition until the skewness of the velocity derivative reaches a physical value of about -0.5 after about 0.2 turnover times. At this stage, particles are seeded into the domain randomly, each with a velocity equal to the local fluid velocity. Three Stokes numbers τ_p/τ_{η_0} are considered in this work, $\mathrm{St}_{\eta,0} \in [3.5, 10, 100]$, where η_0 is the Kolmogorov scale calculated based on the initial condition. At the time of the particle seeding, the turbulence has less energy than initially, and as a consequence, the Stokes numbers at seeding are about 25% below the nominal value. After the particles are seeded, the simulations are continued for at least four turnover times. To examine the effect of turbulence modification, we run three unladen simulations, one for each resolution, to compare to the fluid statistics observed in the presence of particles. The mass loading ratio, ϕ_m, is unity for all particle cases which is a regime expected to have significant two-way coupling effects [42]. The suspension is considered dilute, with the volume fraction $\phi < 10^{-3}$ for all cases. For this reason, we have neglected particle collisions. The particle size is sub-Kolmogorov for all cases, $d_p/\eta_0 \approx 0.25$. In addition, the density ratio for all cases is greater than one thousand. These two conditions together justify the assumption that particles obey Stokes drag. For each Stokes number, we explore cases where our correction scheme is used to estimate the undisturbed fluid velocity against standard interpolation-projection methods including the trilinear, Lagrange-4, and Cubic-Spline schemes while also examining the effect of fluid grid refinement on the predictions of these respective schemes.

In the results section, we report fluid and particle energetics and particle acceleration. For brevity, we omit some of the intermediate Stokes number results which are qualitatively similar to the low

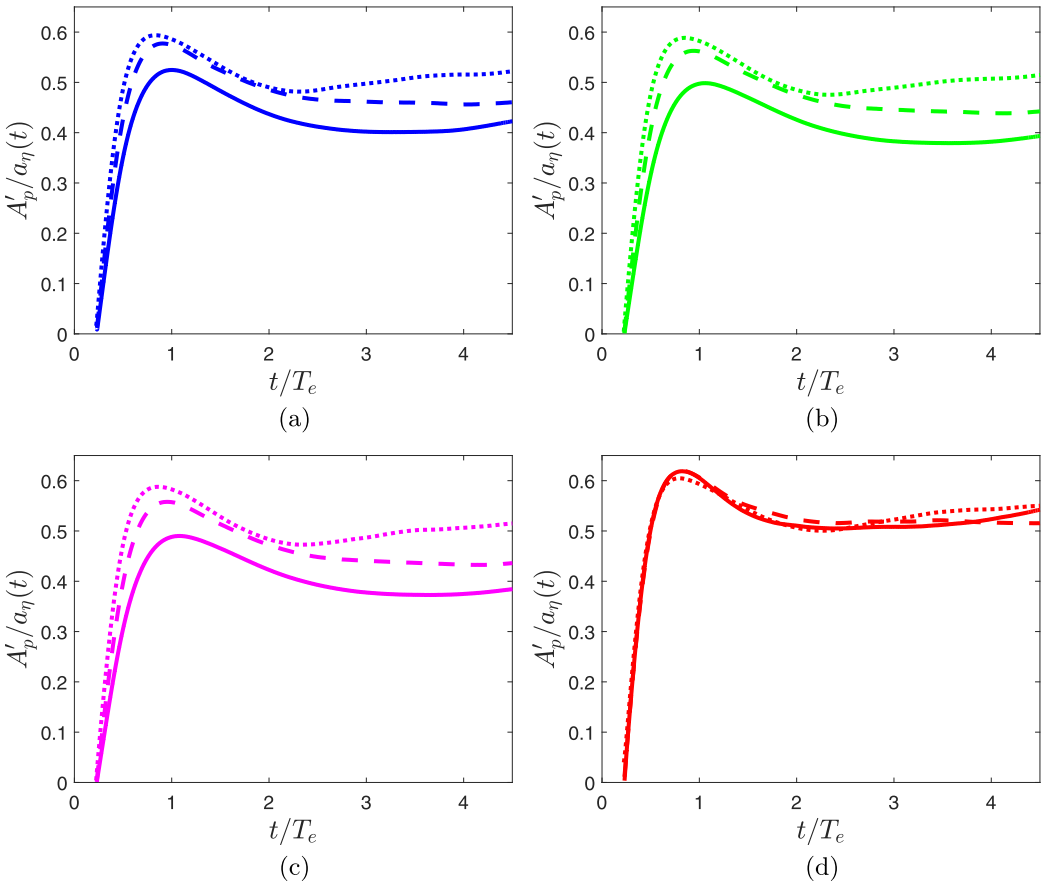

FIG. 1. Particle rms acceleration normalized by unladen Kolmogorov acceleration, showing effect of grid refinement, $\mathrm{St}_0 = 3.5$, (a) Lagrange-2, (b) Lagrange-4, (c) Cubic-Spline, (d) Correction scheme. Different lines show different grid resolutions: dotted-coarse, dash-medium, solid-fine.

Stokes number results. These omitted results can be found in the first author's dissertation [43]. We forgo presenting sensitive quantities such as energy spectra owing to contamination from the two-way coupling disturbance. As a surrogate, we report velocity derivative statistics to demonstrate that giving physical meaning to fine-scale statistics in two-way coupled point-particle simulations should be done so with extreme caution.

A. Particle acceleration

The direct effect of different procedures to calculate fluid velocity in Stokes drag is to vary the drag force each particle experiences as well as the reaction force the fluid feels. Particle rms acceleration is shown in Figs. 1 and 2 for different Stokes numbers and grid resolutions, where the predictions of the proposed correction are compared against standard interpolation-projection schemes. The particle accelerations have been normalized by the Kolmogorov acceleration $a_\eta(t) = u_\eta(t)/\tau_\eta(t)$ of the corresponding unladen simulation at the same grid resolution. This normalization allow us to assess whether the decay rate of particle acceleration eventually matches the decay rate in the acceleration of fluid elements. For each interpolation-projection method, we also show the effect of grid refinement while keeping all other parameters constant.

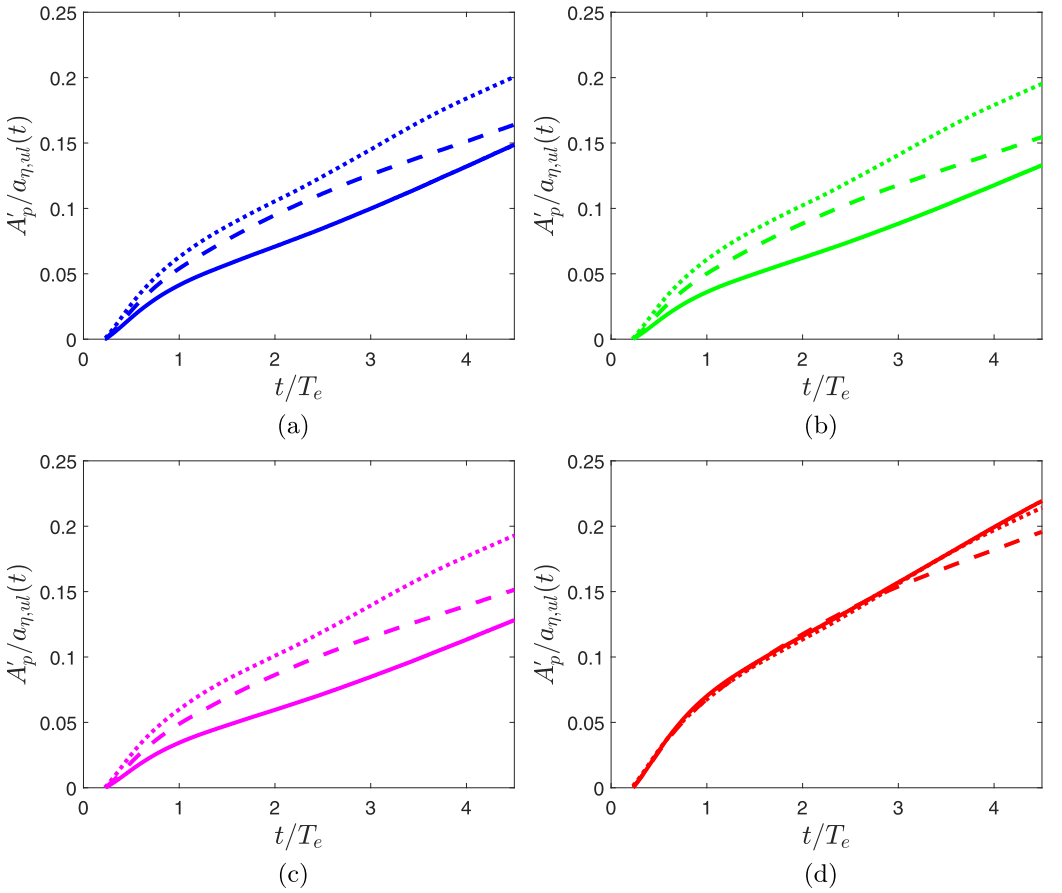

FIG. 2. Particle rms acceleration normalized by unladen Kolmogorov acceleration, showing effect of grid refinement, $\mathrm{St}_0 = 100$, (a) Lagrange-2, (b) Lagrange-4, (c) Cubic-Spline, (d) Correction scheme. Different lines show different grid resolutions: dotted-coarse, dash-medium, solid-fine.

In examining the particle rms acceleration of standard interpolation-projection schemes, [Figs. 1(a)–1(c) and 2(a)–2(c)], it is clear that none of these schemes converge under grid refinement, for any Stokes numbers considered, at any nondimensional time. In contrast, the correction scheme shows no great grid sensitivity for any of the Stokes numbers investigated. No variation is apparent in particle rms acceleration predicted by the correction scheme for about the first turnover time for the lower Stokes numbers, while for the $\mathrm{St}_0 = 100$ case, the correction scheme shows almost no variation with grid resolution for almost three turnover times. At late times there is some modest variation with grid refinement for the correction scheme for each of the Stokes numbers. However, close inspection reveals the coarsest and finest grids are in closest agreement for the correction scheme, suggesting this scheme is making a relatively grid-insensitive prediction of the particle acceleration rather than merely a slower divergence with grid refinement compared with the standard interpolation-projection schemes.

Besides the nonconvergence of particle acceleration under grid refinement using standard interpolation-projection schemes, the main trend is for the magnitude of the particle acceleration to decrease with grid refinement for each of these schemes. Consequently, point particles employing standard interpolation-projection routines will feel less coupled to fluid motion and the fluid will feel less influence of the particle force than they would had the drag force been calculated correctly using

the undisturbed fluid velocity. This observation of less coupling could be interpreted qualitatively as an artificial increase in the effective Stokes number observed when simulations are performed with standard interpolation-projection schemes. In other words, when simulating point particles with standard interpolation-projection schemes, if the nominal Stokes number based on τ_p and τ_η is X, the *simulated* Stokes number using these procedures will be X + a little bit. These results appear consistent with our previous observations [26] that point particles (with $\mathrm{St} > 1$) in two-way coupled forced turbulence obeying standard interpolation-projection schemes showed narrower acceleration PDFs and lower preferential concentration than did point particles computed with the undisturbed fluid velocity, hence underscoring the artificially inflated Stokes numbers predicted by standard interpolation-projection schemes.

Interestingly, the point-particle schemes employing standard interpolation-projection find the best agreement with the correction scheme when the former schemes are employed on coarse grids. To clarify, the coarse grid was chosen as the grid resolution needed to resolve the Kolmogorov scale, and we have chosen a slightly more conservative $k_{\max}\eta$ than suggested in [40] owing to the finite difference solver employed in this work. The virtue of examining finer grids here draws connection to problems requiring stricter resolution of higher moments of the velocity field [44]. Though the difference is nominal, the trilinear scheme shows slower divergence with grid refinement than Lagrange-4 and Cubic-Spline schemes, consistent with the observations of [22] and [30] that lower-order interpolation-projection schemes perform better under laminar conditions in the absence of a correction scheme. The closest agreement between coarse interpolation-projection and correction scheme results presented here combined with the good agreement of the correction scheme against particle-resolved simulations [6] suggests that reducing two-way coupling error at the cost of lower resolution of small scales may be a worthy tradeoff when performing particle-turbulence simulations with uncorrected point-particle schemes.

Finer model appraisal can be ascertained by examining particle acceleration probability density functions (PDFs). Acceleration pdfs comparing performance of the correction scheme with Cubic-Spline scheme at two times are shown in Figs. 3 and 4. The PDFs for the trilinear and Lagrange-4 schemes are qualitatively similar to the Spline predictions and are not shown for brevity. In comparing the uncorrected and corrected acceleration pdfs, it is clear that not only are the uncorrected PDFs narrower than the corrected schemes', the uncorrected PDFs become narrower with grid refinement. Higher acceleration events become monotonically less likely with grid refinement while lower magnitude acceleration events become more probable when the undisturbed fluid velocity is not explicitly modeled. In contrast, the corrected pdfs are remarkably stable to grid refinement for each Stokes number. No discernible variation can be observed in the lower magnitude acceleration events while some nominal variation is observed in the higher acceleration events. However, the trend is not monotonic with grid refinement so the correction scheme does not exhibit bias in its prediction of acceleration events in the PDF tails. These observations surrounding the respective schemes' predictions are reflected throughout the turbulence decay. Interestingly, the Spline predictions for $\mathrm{St}_{\eta,0} = 10$ [Fig. 4(b)], shows little variation with grid refinement for low magnitude acceleration events, however this appears coincidental as the rms acceleration curves shown in the inset appear to have similar magnitudes at this time despite the overall trend of these curves being nonconvergent with grid refinement. The present observations extend the findings in [26] showing explicitly the effect of grid refinement on the PDFs of particle acceleration. Though the shape of the acceleration pdfs and trend of acceleration rms with Stokes number are in qualitative agreement with forced one-way coupled observations [45] at higher turbulence Reynolds number, it is difficult to make a direct quantitative comparison of the present work with available literature owing to the (1) relatively low flow Reynolds number, (2) decaying turbulence, (3) two-way coupling (high mass loading). We note that a direct comparison of point and fully-resolved particles has been performed recently [6], where the point particles incorporated the present correction scheme and when combined with an appropriate drag model produced particle acceleration PDFs in fairly good agreement with the PDFs predicted by the fully resolved particle simulations.

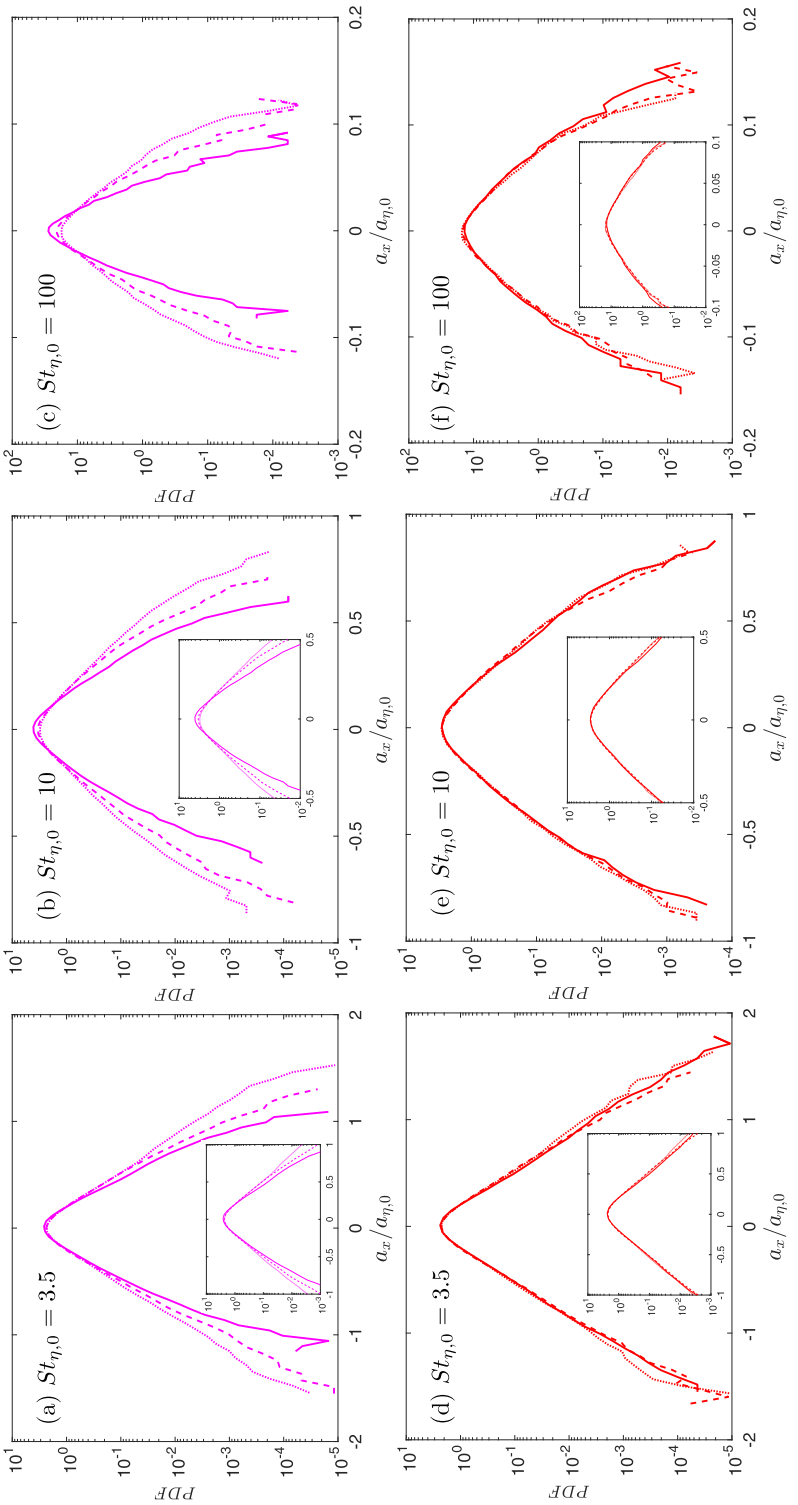

FIG. 3. Particle acceleration PDFs for different Stokes numbers extracted at $t/T_e \approx 1.3$, (a–c) Cubic-Spline, (d–f) correction scheme. Insets show grid refinement collapse/divergence near PDF centers.

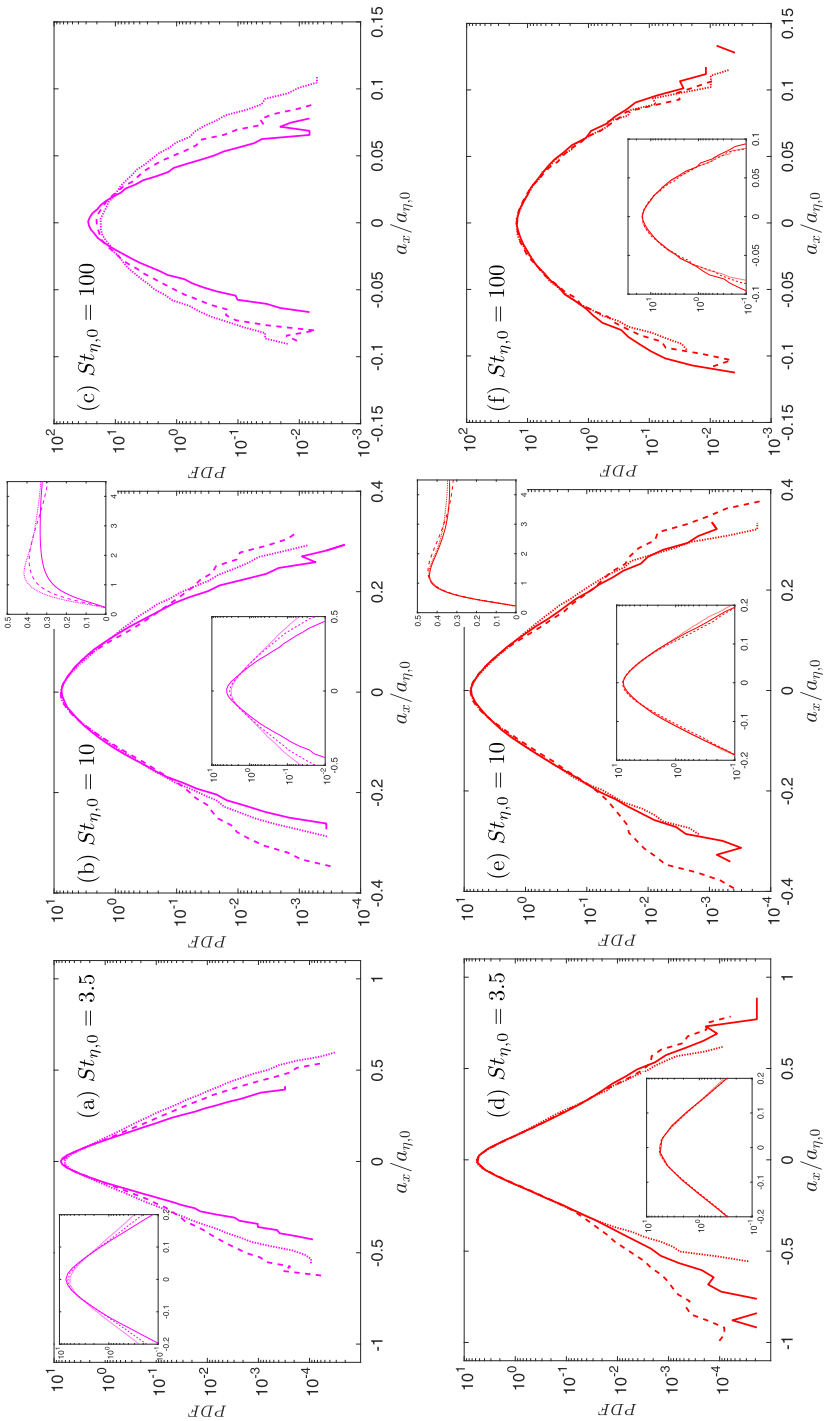

FIG. 4. Particle acceleration PDFs for different Stokes numbers extracted at $t/T_e \approx 3.2$, (a–c) Cubic-Spline, (d–f) correction scheme. Insets show grid refinement collapse/divergence near PDF centers. Additional insets for the $\mathrm{St}_{\eta,0} = 10$ cases show rms acceleration vs time to explain the apparent collapse of the Cubic-Spline scheme with grid refinement. Normalization for the rms acceleration histories is the same as given in Figs. 1 and 2.

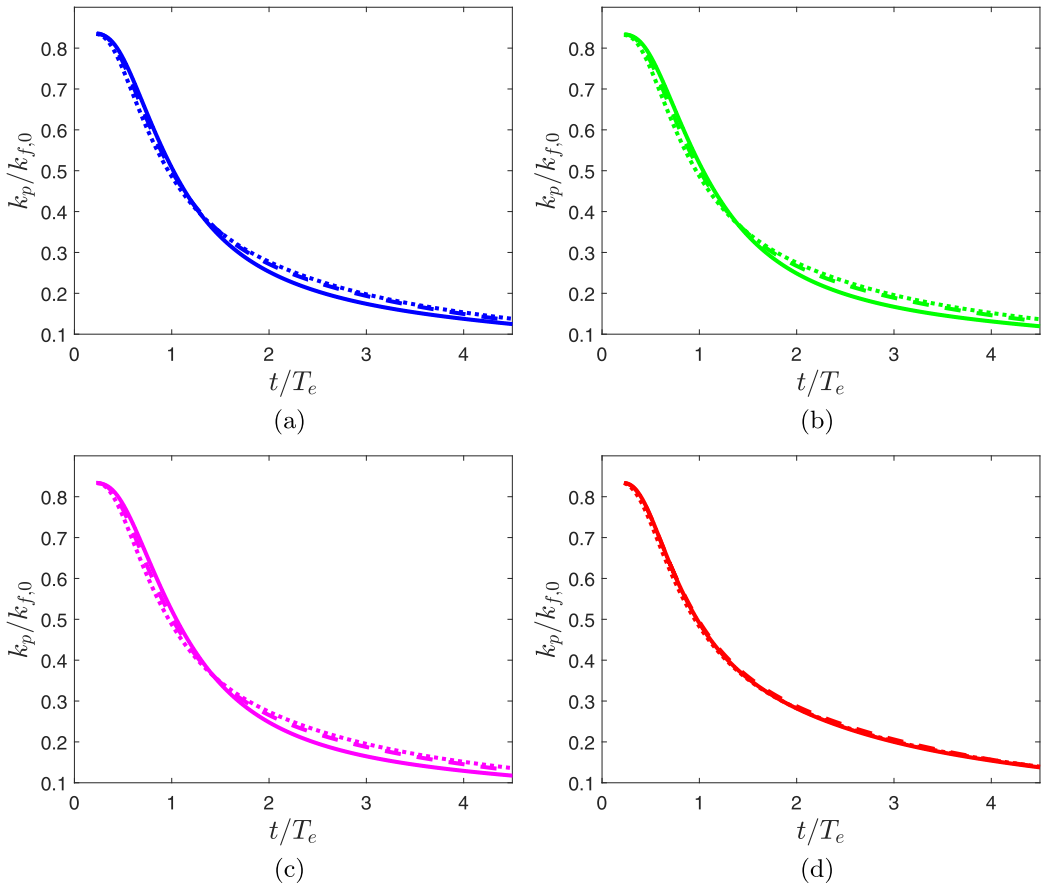

FIG. 5. Particle kinetic energy normalized by initial fluid kinetic energy showing effect of grid refinement, $\mathrm{St}_0 = 3.5$, (a) Lagrange-2, (b) Lagrange-4, (c) Cubic-Spline, (d) Correction scheme. Different lines show different grid resolutions: dotted-coarse, dash-medium, solid-fine.

B. Particle kinetic energy

Figures 5 and 6 show particle kinetic energy for different Stokes numbers and grid resolutions, comparing the predictions of the correction scheme against standard interpolation-projection schemes. Because the unladen simulations are free of particles, we choose to normalize the particle kinetic energy by the initial fluid energy. At seeding, the particle kinetic energy is equal to the instantaneous fluid energy, which is a little over 80% of the initial fluid energy.

In examining Figs. 5 and 6, no significant variation is observed under grid refinement of the particle kinetic energy predicted by the correction scheme for any of the Stokes numbers considered. In contrast, the standard interpolation-projection schemes show grid sensitivity for all Stokes numbers. While the sensitivity is modest at $\mathrm{St}_0 = 3.5$, it is clear that refinement predicts monotonically more particle kinetic energy at early times, and less at late times, where no such variation with grid refinement is observed with the correction scheme. For $\mathrm{St}_0 = 10$ and $\mathrm{St}_0 = 100$, the standard schemes predict higher particle kinetic energy at all times with increasing grid refinement. Since the standard schemes predict lower acceleration (higher Stokes numbers) for a given nominal Stokes number under grid refinement, these uncorrected particles will behave more inertially and retain the kinetic energy associated with their initial condition for longer than they would had their drag been computed correctly by accounting for the undisturbed fluid velocity in a grid-insensitive way.

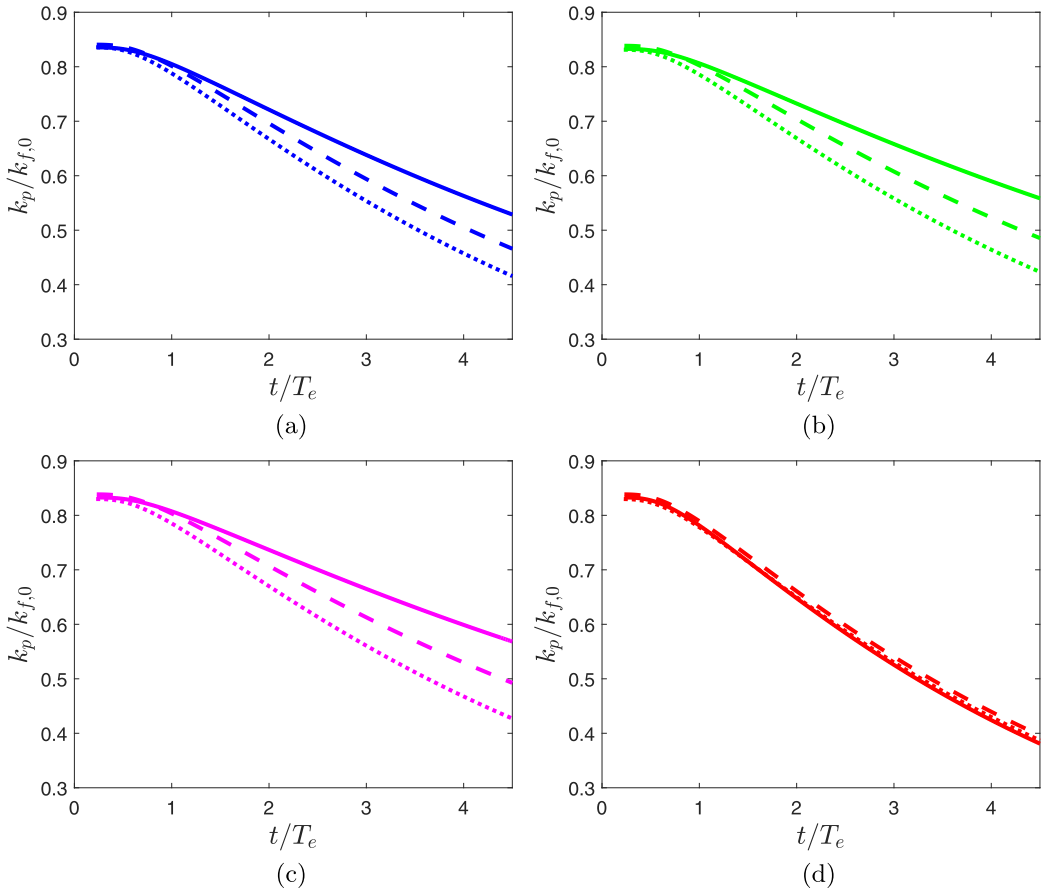

FIG. 6. Particle kinetic energy normalized by initial fluid kinetic energy showing effect of grid refinement, $\mathrm{St}_0 = 100$, (a) Lagrange-2, (b) Lagrange-4, (c) Cubic-Spline, (d) Correction scheme. Different lines show different grid resolutions: dotted-coarse, dash-medium, solid-fine.

C. Turbulence kinetic energy

In Figs. 7 and 8 we show fluid kinetic energy of the particle-laden simulations for different Stokes numbers and grid resolutions, comparing the predictions of the standard interpolation-projection schemes against the correction method. In these figures, the fluid energy of the laden cases k_f at a given mesh resolution has been normalized by the corresponding fluid energy of the unladen simulation $k_{f,ul}(t)$ at the same resolution. We may then define the deviation of the normalized fluid kinetic energy from unity as a measure of turbulence modification. Even though each grid resolution formally corresponds to a different realization of the same turbulent flow (the initial conditions have the same spectrum but are pointwise different velocity fields), our goal here is to show that the errors resulting from inaccurate interpolation projection of the drag force will dominate the variation that results from simulating different realizations of the same turbulence on finer grids. In addition, normalizing by the unladen simulations will allow us to assess whether the particle-laden simulations eventually reach a state where they are decaying at the same rate as the unladen simulations.

In examining the laden fluid energy predicted by standard interpolation-projection schemes (Lagrange-2, Lagrange-4, Cubic-Spline), it is clear that none converge with mesh refinement for any Stokes number. In addition, with the exception of the $\mathrm{St}_0 = 3.5$ cases, none of these schemes

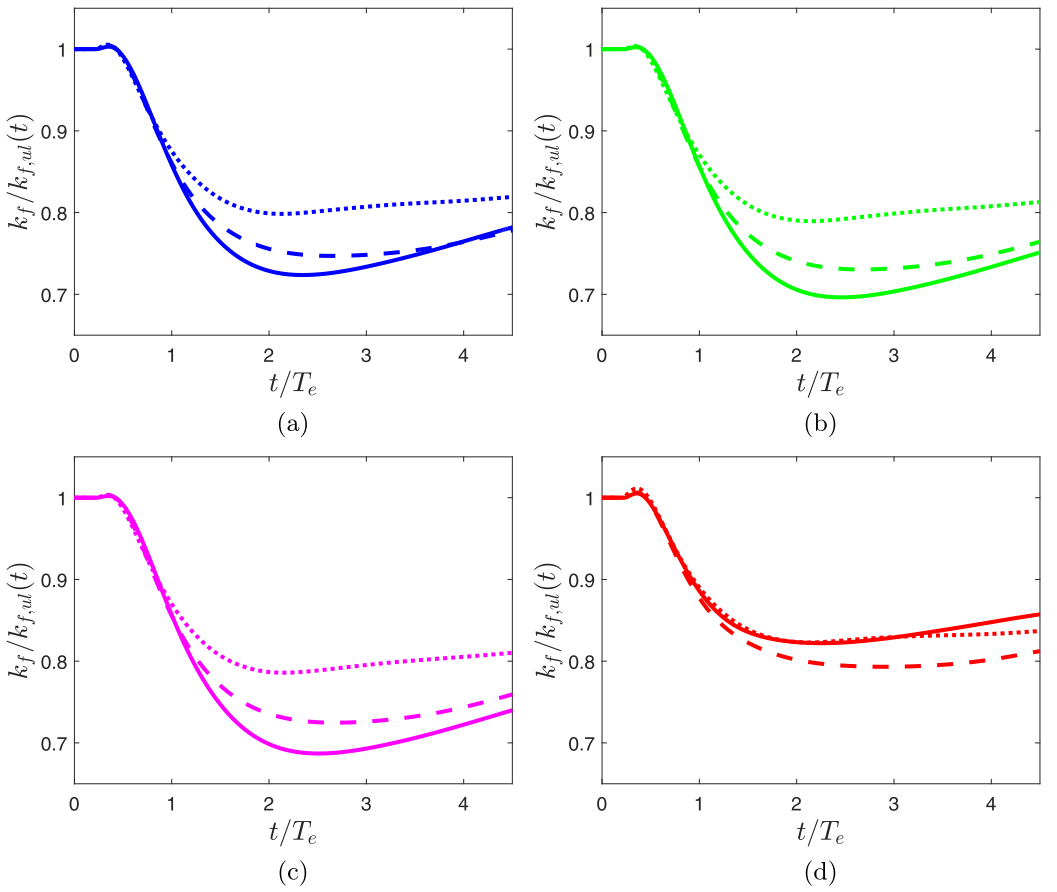

FIG. 7. Fluid kinetic energy of particle-laden cases normalized by unladen fluid energy showing effect of grid refinement, $\mathrm{St}_0 = 3.5$, (a) Lagrange-2, (b) Lagrange-4, (c) Cubic-Spline, (d) Correction scheme. Different lines show different grid resolutions: dotted-coarse, dash-medium, solid-fine.

predict convergence in fluid energy even at early times. As was observed for particle acceleration and kinetic energy, the fluid energy predicted by Lagrange-2 interpolation projection diverges less rapidly with grid refinement, while Cubic-Spline and Lagrange-4 exhibit greater divergence. In contrast, the statistics of laden fluid energy predicted by the correction scheme in Figs. 7(d) and 8(d), show relative insensitivity to the choice of grid. In particular, Fig. 7(d) clearly demonstrates grid convergence at early times with modest variation at late times. Similar late time variation was also observed for rms particle acceleration predicted by the correction scheme. We suspect this late time behavior is partially a consequence of the realization effect. At late times in the simulation, most of the little remaining fluid energy is associated with small wave number big eddies, which are most likely to be realization-dependent. It is worth noting that the fluid energy predicted by the correction scheme for the highest Stokes number [Fig. 8(d)] shows no discernible variation among the three grid resolutions. The realization effect may not be observable here since the particle relaxation time for the highest Stokes number is considerably longer than the eddy turnover time. For this Stokes number, observing the realization effect would require sufficiently large eddies with timescale comparable to the particle relaxation time; this would require a much larger simulation domain. This high Stokes number case in particular demonstrates the divergence in fluid energy is a result of not robustly modeling the undisturbed fluid velocity in the particle drag. The finest

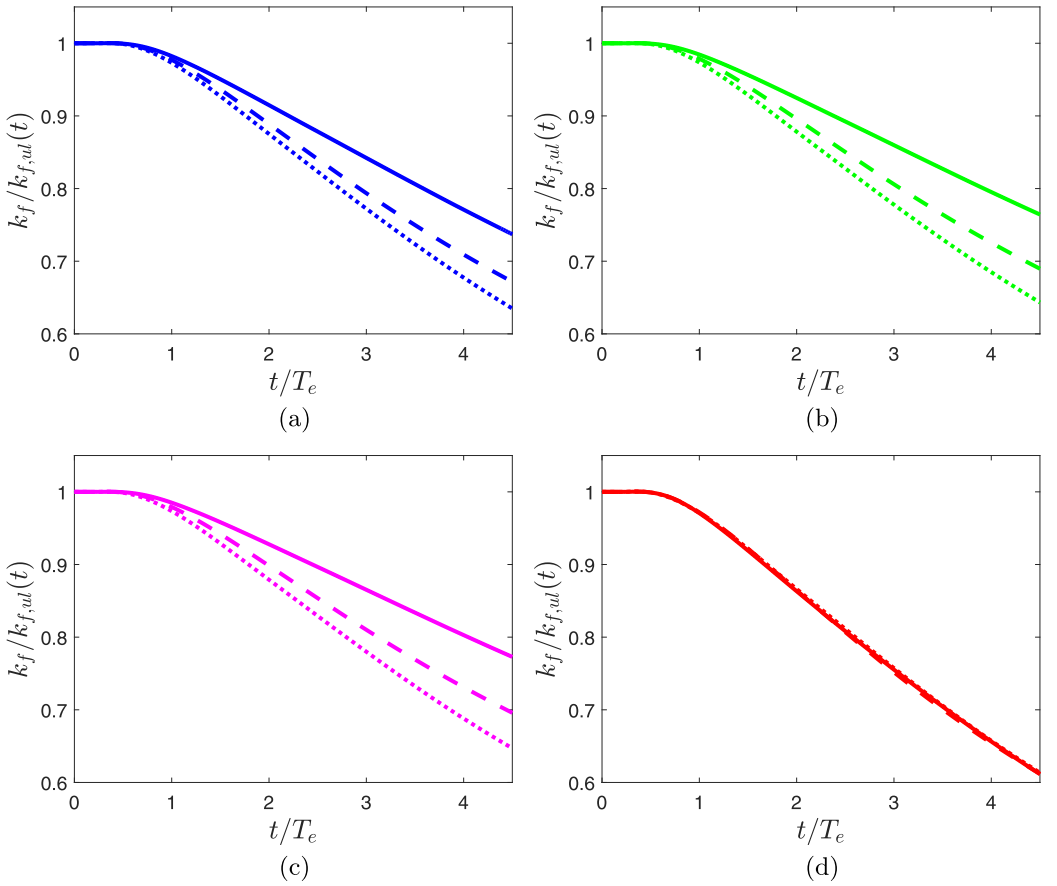

FIG. 8. Fluid kinetic energy of particle-laden cases normalized by unladen fluid energy showing effect of grid refinement, $\mathrm{St}_0 = 100$, (a) Lagrange-2, (b) Lagrange-4, (c) Cubic-Spline, (d) Correction scheme. Different lines show different grid resolutions: dotted-coarse, dash-medium, solid-fine.

grid solutions of the standard interpolation-projection schemes have approximately 15% more fluid energy at late times than that predicted by the correction scheme. As we have observed for the other statistics, the coarsest grid solutions of standard interpolation-projection schemes best predict the results of the correction scheme, with the Lagrange-2 scheme being the least inaccurate method not incorporating an explicit model for the undisturbed fluid velocity.

D. Turbulence dissipation rate: Demonstration of the correspondence principle

The previous sections have demonstrated that incorporation of an explicit estimate for the undisturbed fluid velocity yields relatively grid-insensitive predictions of particle and fluid kinetic energy. Therefore, it may be expected that a similar conclusion should apply to the fluid dissipation rate. This hypothesis is correct, provided we are careful to specify which dissipation rate should be grid-insensitive. Starting from the Navier-Stokes equation for the fluid and the momentum balance for each particle, the evolution equation governing the mixture energy of the system

$e_m = (1-\phi)\rho_f k_f + \phi\rho_p k_p$ is [6]

$$\frac{de_m}{dt} = -\varepsilon_f + \frac{1}{V}\sum_{i=1}^{N_p} \mathbf{F}_i \cdot [\mathbf{v}_i - \mathbf{u}_f(\mathbf{x}_i)] + \phi\frac{1}{V}\sum_{i=1}^{N_p} \mathbf{F}_i \cdot \mathbf{u}_f(\mathbf{x}_i). \tag{6}$$

In Eq. (6), $-\varepsilon_f = (1-\phi)(1/V)\int_V \mu \mathbf{u}_f \nabla^2 \mathbf{u}_f \, dV$, is the fluid dissipation rate which is resolved on the fluid grid, with V being the whole fluid volume. The remaining two terms in Eq. (6) comprise an additional particle-dissipation rate [22,23]. The particle-dissipation rate can be interpreted as an additional dissipation rate owing to the point-particle model. In particle-resolved simulation, all of the fluid dissipation rate appears in the ε_f term and there is no particle-dissipation term [6,7]. Therefore the additional particle-dissipation rate term can be interpreted as a compensation to the resolved dissipation rate since not all of the true fluid dissipation of the system is being resolved on the fluid grid. In a direct comparison of point particles against fully resolved particles [6], it was verified that both the dissipation rate resolved on the fluid grid and the additional particle dissipation together should be compared to the viscous dissipation rate obtained from the particle-resolved simulation. Further, it was shown that with an explicit estimate for the undisturbed fluid velocity and an appropriate drag model for the point particles, the sum of the resolved and additional dissipation rate in the point-particle simulation showed excellent agreement with the particle-resolved simulation.

In Figs. 9–11 we show the total dissipation rate (sum of resolved and additional dissipation) as well as resolved dissipation rate for the various interpolation-projection schemes. Note, the dissipation results presented here consider one to three orders of magnitude more particles depending on the Stokes number than the $O(10^3)$ particles considered in [6]. The results here have been normalized by the viscous dissipation of the unladen simulations at the same resolution. The *total* dissipation rate for the standard interpolation-projection schemes is highly grid sensitive while for the correction scheme, nominal variation in total dissipation is observed for a given Stokes number on different grids. It is important to remark that the *resolved* dissipation rate is highly grid sensitive for both correction and noncorrection schemes. For example, in considering the coarse grid for the $\mathrm{St}_0 = 10$ and 100 cases, one could erroneously conclude that the (resolved) dissipation rate for the particle-laden suspension is lower than for the unladen suspension. At least for the cases considered here, we see that the total (true) dissipation rate is in fact always greater than for the unladen suspension. This observation underscores the point that the resolved fluid dissipation rate should never be reported as indicative of the true (total) fluid dissipation rate of the mixture energy of the system. As the resolved viscous dissipation rate changes significantly with grid refinement, so too does the particle-source term (shown in the insets). These observations suggest that neither the resolved dissipation nor particle-dissipation terms extracted from point-particle simulation should ever be reported alone. They are not physically meaningful by themselves. Rather, each of these terms varies in such a way that with grid refinement, their sum is grid-insensitive, with the proper incorporation of an undisturbed fluid velocity correction.

We call these collective observations the *correspondence principle*. Using a point-particle method does not guarantee a pointwise convergent velocity field to a particle-resolved simulation. The no-slip boundary condition cannot be enforced for point particles, nor are the velocity gradient structures found in a point-particle simulation statistically identical to those found in a particle-resolved simulation. However, incorporation of the proper drag model for point particles combined with a good estimate for the undisturbed fluid velocity implies a total dissipation rate (which can be compared to a particle-resolved simulation) which is grid-insensitive. The results presented here regarding grid insensitivity of total dissipation rate in a time-evolving flow combined with the validation of this corrected point-particle method against a particle-resolved simulation in decaying turbulence [6] are particular noteworthy. We had previously demonstrated the correspondence principle under laminar conditions [22]. In that work, we showed analytically that a settling point particle would dissipate the correct amount of energy consistent with the drag law chosen if an accurate undisturbed fluid velocity correction is adopted. That is, a Stokesian particle should,

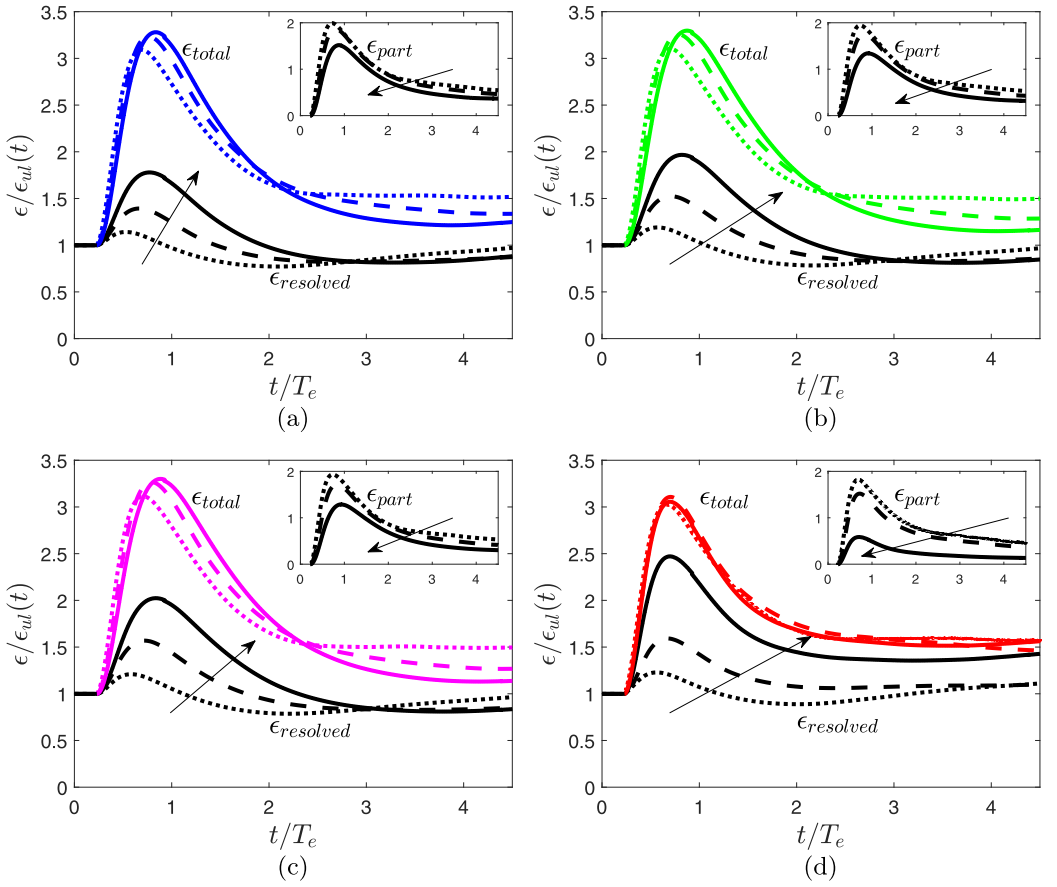

FIG. 9. Total and resolved fluid dissipation rate of particle-laden cases normalized by unladen fluid dissipation rate showing effect of grid refinement, $\mathrm{St}_0 = 3.5$, (a) Lagrange-2, (b) Lagrange-4, (c) Cubic-Spline, (d) Correction scheme. Different lines show different grid resolutions: dotted-coarse, dash-medium, solid-fine. The insets show the particle dissipation term.

in *steady state*, dissipate an amount of an energy per unit time consistent with the Stokes drag model. The same applies for the dissipation rate for a Schiller-Naumann particle for example. The observations here, combined with the particle-resolved comparison study [6], shows that the steady correspondence principle [22] may in fact apply to time-evolving flows. Though this hypothesis should be explored in more detail, we suspect that, in the case of highly unsteady flows or big particles such that history terms are important in describing the particle equation of motion, a correspondence principle may be satisfied if the particle drag force is evaluated with suitable corrections to the undisturbed history terms; see, e.g., [15]. Nevertheless, it remains an open question whether there is a cutoff particle Reynolds number above which no correspondence should be expected. In other words, at high enough particle Reynolds number, vortex recirculation or shedding will occur and it seems that it would be difficult for a point model (even with an appropriate drag-formulation and undisturbed-quantity corrections) to be able to recover critical dissipation events occurring in particle wakes.

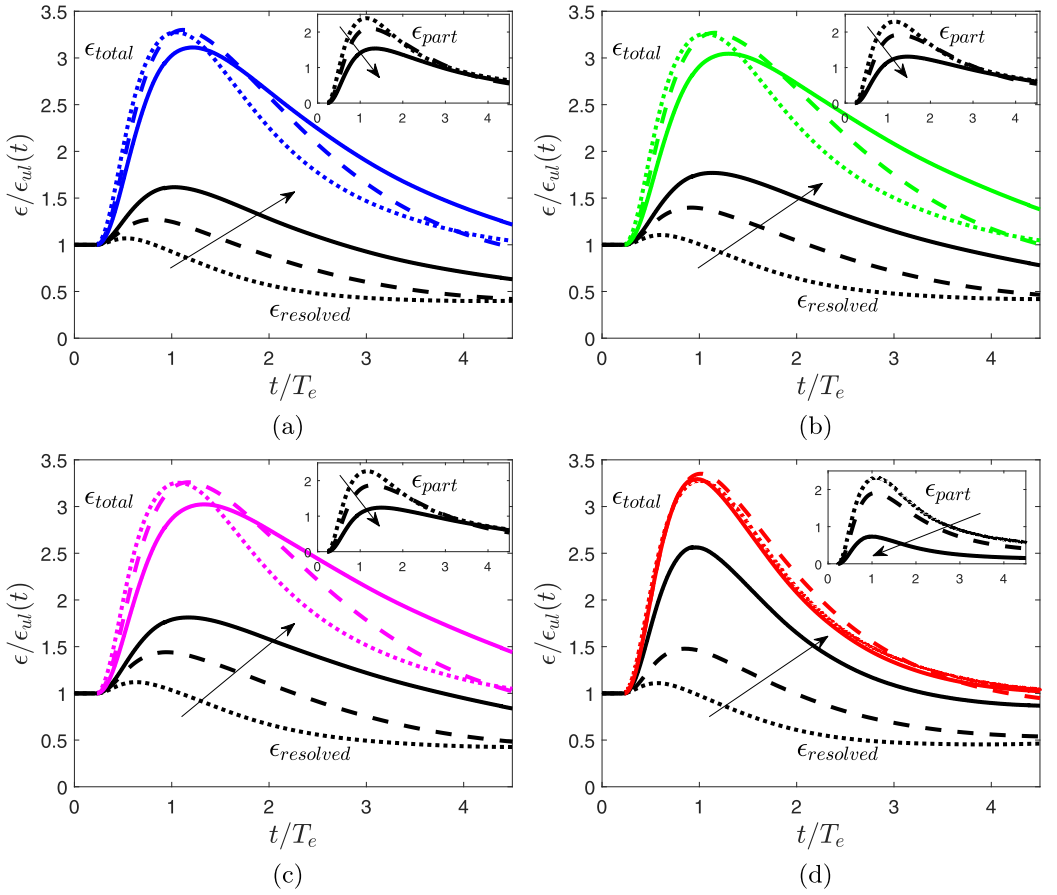

FIG. 10. Total and resolved fluid dissipation rate of particle-laden cases normalized by unladen fluid dissipation rate showing effect of grid refinement, $\mathrm{St}_0 = 10$, (a) Lagrange-2, (b) Lagrange-4, (c) Cubic-Spline, (d) Correction scheme. Different lines show different grid resolutions: dotted-coarse, dash-medium, solid-fine. The insets show the particle dissipation term.

E. Higher-order statistics

The previous results provide insight into what can be reasonably expected from a point-particle method. Within the scope of the model problem chosen and the Stokes numbers considered, accurate estimation of the undisturbed fluid velocity yielded relatively grid-insensitive particle acceleration, fluid, and particle energy. In addition, the total dissipation rate was found to be grid-insensitive when an explicit model for the undisturbed fluid velocity was adopted. However, the resolved fluid dissipation rate was found to be grid sensitive for all interpolation-projection schemes. This observation serves as a harbinger for the results in this section.

In this section, we focus on the skewness $S = \overline{(\frac{\partial u_1}{\partial x_1})^3}/[\overline{(\frac{\partial u_1}{\partial x_1})^2}]^{3/2}$, and kurtosis $K = \overline{(\frac{\partial u_1}{\partial x_1})^4}/[\overline{(\frac{\partial u_1}{\partial x_1})^2}]^2$ of the velocity derivative. The skewness is related to the behavior of the two-point correlation function at intermediate separations [46] as well as the distribution of vortex tubes and sheets in the flow [47] while the kurtosis characterizes flow intermittency. To anticipate that particles will modify velocity-derivative statistics, we report the evolution equation for the unnormalized nth moment of the velocity derivative under homogeneous, zero-mean conditions. This equation can be derived by taking the gradient of the point-particle equations (1), taking the $1-1$ component of the

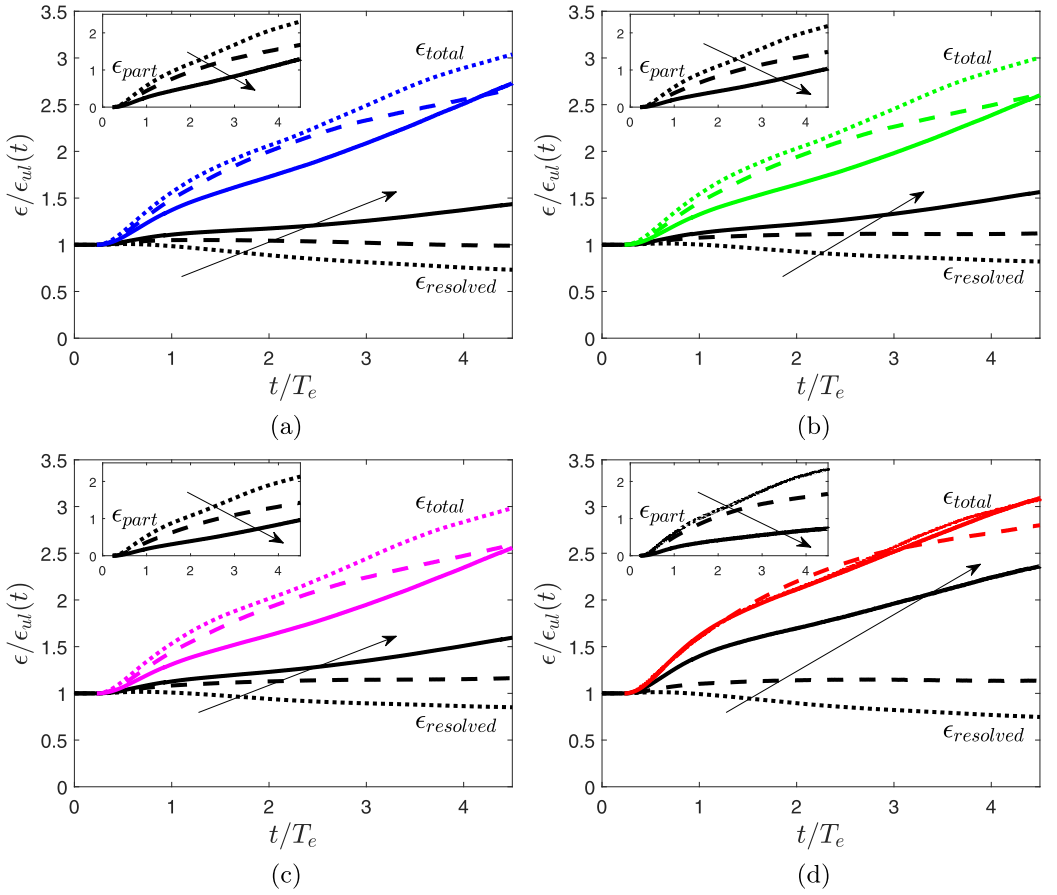

FIG. 11. Total and resolved fluid dissipation rate of particle-laden cases normalized by unladen fluid dissipation rate showing effect of grid refinement, $\mathrm{St}_0 = 100$, (a) Lagrange-2, (b) Lagrange-4, (c) Cubic-Spline, (d) Correction scheme. Different lines show different grid resolutions: dotted-coarse, dash-medium, solid-fine. The insets show the particle dissipation term.

resulting equation, then multiplying through by $n(\frac{\partial u_1}{\partial x_1})^{n-1}$ and ensemble averaging yields

$$\frac{\partial}{\partial t}\overline{Z}_n + n\overline{Z_{n-1}\frac{\partial u_j}{\partial x_1}\frac{\partial u_1}{\partial x_j}} = -n\overline{Z_{n-1}\frac{\partial^2 p/\rho_f}{\partial x_1 \partial x_1}} - \nu n(n-1)\overline{Z_{n-2}\frac{\partial Z_1}{\partial x_j}\frac{\partial Z_1}{\partial x_j}} + n\overline{Z_{n-1}\frac{\partial f_1}{\partial x_1}}. \tag{7}$$

In Eq. (7), $\overline{Z}_n$ is the unnormalized nth moment of the velocity derivative, with $Z_n = (\frac{\partial u_1}{\partial x_1})^n$, and f_1 is the 1-component of a forcing term owing to particle two-way coupling.

The effect of grid refinement on velocity derivative skewness and kurtosis in the unladen simulations are demonstrated in Figs. 12(a) and 12(b). The unladen skewness appears to exhibit nominal changes with grid refinement. The variation may be attributed to stricter resolution requirements for higher moments [44] as well as the different realizations of the initial conditions on different grids. Overall, this gives a baseline for the amount of variation which may be expected from grid refinement versus the variation of skewness which will be owing to the particles.

Velocity derivative skewness for the laden simulations is shown in Fig. 13. It is most evident when examining the $\mathrm{St}_0 = 10$ and $\mathrm{St}_0 = 100$ cases that the velocity derivative skewness is slowly diverging with grid refinement for all interpolation-projection schemes. This implies that the

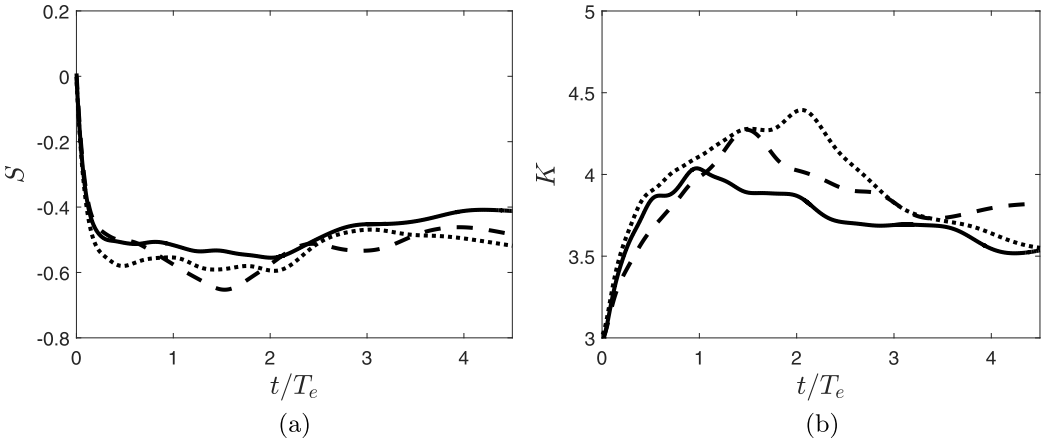

FIG. 12. Velocity derivative (a) skewness and (b) kurtosis of the unladen simulations. Different lines show different grid resolutions: dotted-coarse, dash-medium, solid-fine.

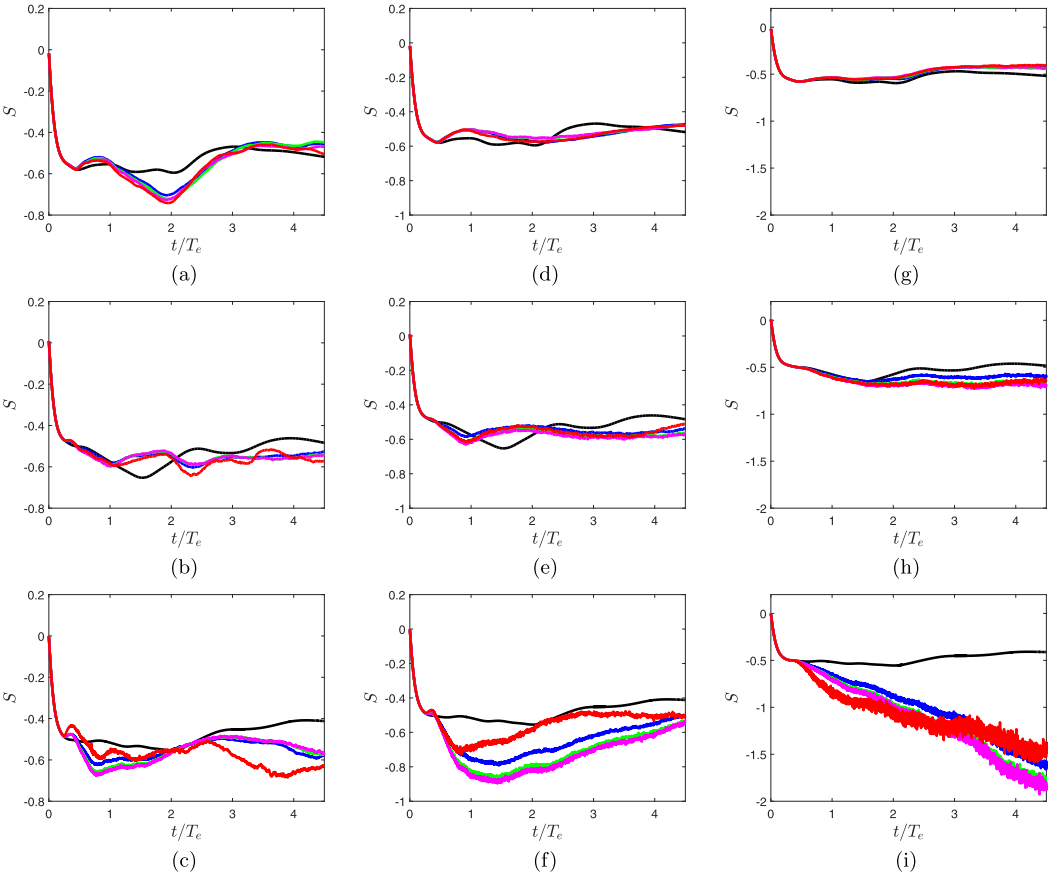

FIG. 13. Velocity derivative skewness from particle-laden simulations for different Stokes numbers, (a–c) $St_0 = 3.5$, (d–f) $St_0 = 10$, (g–i) $St_0 = 100$; each column shows variation from coarse to fine grid resolution. Note the differences in magnitude on the ordinates. Colors represent different numerical schemes: blue: Lagrange-2, green: Lagrange-4, magenta: Cubic-Spline, red: Correction scheme, black: unladen.

structures responsible for the energy cascade are grid-dependent, even if for the correction scheme, the total dissipation rate is grid-insensitive. The observation of grid dependence of the resolved dissipation rate in the previous section is consistent with the grid dependence of velocity derivative skewness, since the skewness is a source term for enstrophy, the latter quantity directly proportional to dissipation in homogeneous turbulence.

At present, it is not known whether it is possible to form a correspondence principle for skewness expressed as a resolved plus point-particle model form skewness. The fact that the resolved skewness is related to the distribution of vortex structures in the flow means that these structures are also grid-dependent. Because the distribution and magnitude of these structures are tied to particle preferential concentration, we feel it would behove point-particle modelers to interpret with extreme caution preferential-concentration statistics (especially at small separations) predicted from two-way coupled simulations, especially when the particle size is comparable to or larger than the grid spacing. At small separations, two-way coupled point particles will see their mutual disturbance fields. But these disturbance flows will not have a Stokesian structure even for Stokesian point particles. Rather these disturbance structures in the particle near-fields will have the symmetries endowed by the projection operator used to transfer the particle force to the grid. We suspect this artificial projection step, which is necessary to two-way couple point particles to the fluid, likely causes contamination of two-particle statistics at small separations (even for grid-independent, Gaussian-type projections).

The unladen derivative kurtosis [Fig. 12(b)] shows nominal variation with grid refinement (the peak kurtosis changes by about 10% from coarse to fine simulation). In contrast, the laden velocity derivative kurtosis (Fig. 14) clearly diverges with grid refinement for all schemes and Stokes numbers (note the difference in the values on the ordinates). To make the point most clear, for the finest grid and $\mathrm{St}_0 = 100$, the correction and spline schemes predict kurtosis values exceeding 1000, which is greater than the highest kurtosis ever measured (as of 1980 and in unladen flow), by more than a factor of 10, corresponding to Re_λ in excess of 10 000 [48]. A physical explanation for the increase in kurtosis with time (assuming these simulations model a real particle-laden flow) may be explained by the fact that heavy particles (which hold onto their energy longer than the fluid) are injecting fluctuations into the fluid characteristic of the energy the particles acquired at earlier times. These relatively high velocity fluctuations may show up as rare velocity derivative events. Similarly, it could be argued that collisions present in a real particle-laden flow (but neglected in these simulations) would, under certain filtering of the fluid velocity field predict enhanced kurtosis. However, these collective observations of velocity derivative statistics suggests that certain physical quantities cannot be reliably predicted, at least at present, from point-particle simulations. Another example would be fluid velocity spectra, especially at high wave numbers.

The great dependence of velocity derivative statistics on the fluid grid suggests that the name assigned to the method used to conduct these simulations, Point-Particle Direct Numerical Simulation (PP-DNS), is inappropriate and should no longer be used in the literature. We would like to propose the name "Point-Particle Resolving-if-Unladen Numerical Simulation (PP-RUNS)," which removes the ambiguity that this method represents a direct simulation of particle-laden flow, yet distinguishes it from point-particle large eddy simulation, by acknowledging in the former method that all of the artificial scales are owing to the adoption of a point-force model instead of the latter approach which does not resolve all flow features even in the absence of particles. An alternative name which is amenable to point-particle simulations across various flow resolutions is "PP-Modeled Particle-Fluid Simulation."

IV. CONCLUSION

The main purpose of this work was to understand how different two-way coupling schemes in conjunction with grid-refinement affect the statistics predicted by point-particle simulations. These effects were studied in particle-laden decaying homogeneous isotropic turbulence for three Stokes numbers. Point-particle simulations which did not use an explicit model for the undisturbed fluid

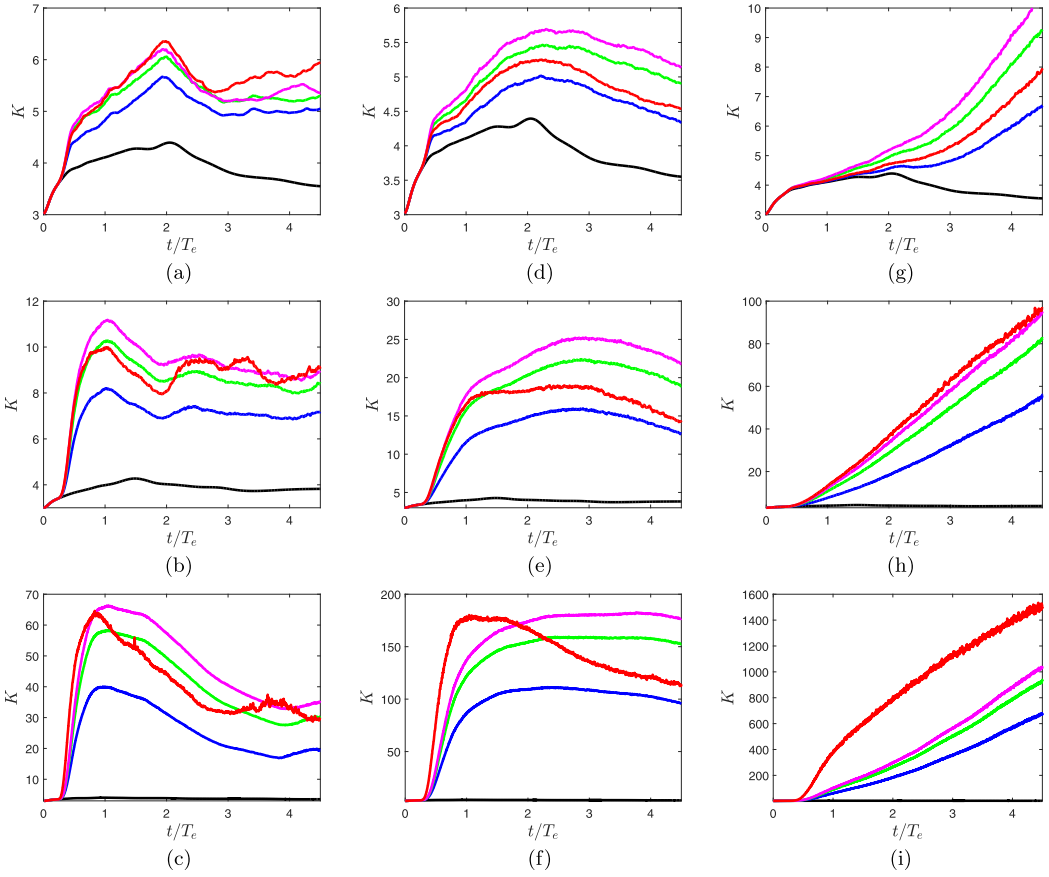

FIG. 14. Velocity derivative kurtosis from particle-laden simulations for different Stokes numbers, (a–c) $\mathrm{St}_0 = 3.5$, (d–f) $\mathrm{St}_0 = 10$, (g–i) $\mathrm{St}_0 = 100$; each column shows variation from coarse to fine grid resolution. Note the differences in magnitude on the ordinates. Colors represent different numerical schemes: blue: Lagrange-2, green: Lagrange-4, magenta: Cubic-Spline, red: Correction scheme, black: unladen.

velocity in the particle-drag force yielded grid-dependent particle and fluid statistics across all of the Stokes numbers studied.

Simulations that incorporated an undisturbed fluid velocity correction scheme yielded grid-insensitive predictions of particle acceleration and kinetic energy, as well as fluid energy. It was also found that the correction scheme predicted grid-insensitive dissipation, provided the dissipation reported is the total dissipation rate (i.e., the sum of the resolved plus particle-dissipation rate). In conjunction with a validation of the correction scheme against a particle-resolved simulation [6], we stated a correspondence principle that point particles satisfy: We propose that for a given particle-resolving simulation, there exists a point-particle model which predicts some of the low-order statistics from the PR-DNS provided the point-particle method incorporates the correct drag model required to capture the physical interactions in the particle-resolving simulation, and the fluid quantities found in the chosen drag law are accurately calculated with an undisturbed fluid velocity correction. In particular the undisturbed velocity correction scheme used in this work is valid for low volume fractions; however, in highly concentrated regimes, directly modeling the influence of particle neighbors on the forces each particle experiences is essential for a point-particle simulation to be predictive [49]. Overall, the correspondence principle stated here has been tested only in simple configurations (laminar flows and homogeneous turbulence). More work should be focused

on inhomogenous settings comparing point and particle-resolved predictions to understand what are reasonable expectations from a point-particle method in these regimes.

Whereas in single-phase turbulence, higher-order statistics can be resolved with a sufficiently refined grid, that may be impossible for two-way coupled point-particle simulations. All point-particle methods studied in this work predicted diverging velocity derivative skewness and kurtosis with grid refinement. Based on these findings, we feel that computational users should interpret small-scale statistics extracted from two-way coupled point-particle simulations with extreme caution. Specifically, we expect that grid-dependent fine-scale structures could yield quantitative mispredictions about the magnitude of preferential concentration at small separations, and the conditional structures correlated with the particle-field.

In spite of the results presented here, we feel point-particle simulations continue to be of value for studying particle-laden flow physics; however, computational modelers should be mindful of what are reasonable questions to study using this methodology, and cautious when interpreting statistics (especially from nonverified two-way coupled simulations). To emphasize the logic usually associated with direct numerical simulation in single phase does not apply to PP-DNS, we propose renaming PP-DNS as PP-RUNS (point-particle resolving-if-unladen numerical simulation). This name makes clear that resolution is chosen to resolve the unladen Kolmogorov scale, yet acknowledges there will be artifacts introduced when a fluid is coupled to a noncontinuum phase modeled by regularized point sources.

ACKNOWLEDGMENTS

We appreciate the anonymous reviewers' constructive comments, which considerably strengthened this paper. Some of these results were presented in a preliminary form at the 2015 APS DFD [50] and the 2016 ICMF [30] and have been documented in J.A.K.H.'s unpublished dissertation [43]. Funding has been provided by the United States Department of Energy through the Predictive Science Academic Alliance Program 2 at Stanford University under Grant No. DE-NA0002373. This work was completed while J.A.K.H. also received support from a National Science Foundation Graduate Research Fellowship under Grant No. DGE-114747. Any opinion, findings, and conclusions or recommendations expressed in this material are those of the authors and do not necessarily reflect the views of the National Science Foundation. This work was performed under the auspices of the US Department of Energy by Lawrence Livermore National Laboratory under Contract No. DE-AC52-07NA27344. LLNL-JRNL-791338.

[1] P. G. Saffman, On the settling speed of free and fixed suspensions, Stud. Appl. Math. **52**, 115 (1973).

[2] G. K. Batchelor, *An Introduction to Fluid Dynamics* (Cambridge University Press, Cambridge, 1967).

[3] S. Tenneti and S. Subramaniam, Particle-resolved direct numerical simulation for gas-solid flow model development, Annu. Rev. Fluid Mech. **46**, 199 (2014).

[4] P. A. Cundall and O. D. L. Strack, A discrete numerical model for granular assemblies, Geotechnique **29**, 47 (1979).

[5] M. Mehrabadi, S. Tenneti, R. Garg, and S. Subramaniam, Pseudo-turbulent gas-phase velocity fluctuations in homogeneous gas-solid flow: Fixed particle assemblies and freely evolving suspensions, J. Fluid Mech. **770**, 210 (2015).

[6] M. Mehrabadi, J. A. K. Horwitz, S. Subramaniam, and A. Mani, A direct comparison of particle-resolved and point-particle methods in decaying turbulence, J. Fluid Mech. **850**, 336 (2018).

[7] S. Subramaniam, M. Mehrabadi, J. Horwitz, and A. Mani, Developing improved Lagrangian point particle models of gas-solid flow from particle-resolved direct numerical simulation, in *Studying Turbulence Using Numerical Simulation Databases-XV, Proceedings of the CTR 2014 Summer Program* (Center for Turbulence Research, Stanford University, 2014), pp. 5–14.

[8] L. Schneiders, M. Meinke, and W. Schroder, Direct particle-fluid simulation of Kolmogorov-length-scale size particles in decaying isotropic turbulence, J. Fluid Mech. **819**, 188 (2017).
[9] W. Fornari, F. Picano, and L. Brandt, Sedimentation of finite-size spheres in quiescent and turbulent environments, J. Fluid Mech. **788**, 640 (2016).
[10] M. Uhlmann and A. Chouippe, Clustering and preferential concentration of finite-size particles in forced homogeneous-isotropic turbulence, J. Fluid Mech. **812**, 991 (2017).
[11] L. Schneiders, K. Frohlich, M. Meinke, and W. Schroder, The decay of isotropic turbulence carrying non-spherical finite-size particles, J. Fluid Mech. **875**, 520 (2019).
[12] A. Ferrante and S. Elghobashi, On the physical mechanisms of two-way coupling in particle-laden isotropic turbulence, Phys. Fluids **15**, 315 (2003).
[13] L. Zhao, H. I. Andersson, and J. J. J. Gillissen, Interphasial energy transfer and particle dissipation in particle-laden wall turbulence, J. Fluid Mech. **715**, 32 (2013).
[14] K. Frohlich, L. Schneiders, M. Meinke, and W. Schroder, Validation of Lagrangian two-way coupled point-particle models in large-eddy simulations, Flow Turbulence Combustion **101**, 317 (2018).
[15] S. Balachandar, K. Liu, and M. Lakhote, Self-induced velocity correction for improved drag estimation in Euler-Lagrange point-particle simulations, J. Comput. Phys. **376**, 160 (2019).
[16] M. Boivin, O. Simonin, and K. D. Squires, On the prediction of gas-solid flows with two-way coupling using large eddy simulation, Phys. Fluids **12**, 2080 (2000).
[17] J. C. Segura, Predictive capabilities of particle-laden large eddy simulation, Ph.D. thesis, Stanford University, 2004.
[18] M. Esmaily and J. A. K. Horwitz, A correction scheme for two-way coupled point-particle simulations on anisotropic grids, J. Comput. Phys. **375**, 960 (2018).
[19] F. Battista, J. P. Mollicone, P. Gualtieri, R. Messina, and C. M. Casciola, Exact regularized point particle (ERPP) method for particle-laden wall-bounded flows in the two-way coupling regime, J. Fluid Mech. **878**, 420 (2019).
[20] J. A. K. Horwitz, G. Iaccarino, J. K. Eaton, and A. Mani, The discrete Green's function paradigm for two-way coupled euler-lagrange simulation, arXiv:2004.08480.
[21] G. G. Stokes, On the effect of the internal friction of fluids on the motion of pendulums, Trans. Cambr. Philos. Soc. **9**, 1 (1850).
[22] J. A. K. Horwitz and A. Mani, Accurate calculation of Stokes drag for point-particle tracking in two-way coupled flows, J. Comput. Phys. **318**, 85 (2016).
[23] S. Sundaram and L. R. Collins, Numerical considerations in simulating a turbulent suspension of finite-volume particles, J. Comput. Phys. **124**, 337 (1996).
[24] P. Gualtieri, F. Picano, G. Sardina, and C. M. Casciola, Exact regularized point particle method for multiphase flows in the two-way coupling regime, J. Fluid Mech. **773**, 520 (2015).
[25] P. J. Ireland and O. Desjardins, Improving particle drag predictions in Euler-Lagrange simulations with two-way coupling, J. Comput. Phys. **338**, 405 (2017).
[26] J. A. K. Horwitz and A. Mani, Correction scheme for point-particle models applied to a nonlinear drag law in simulations of particle-fluid interaction, Int. J. Multiphase Flow **101**, 74 (2018).
[27] H. Pouransari, M. Mortazavi, and A. Mani, Parallel variable-density particle-laden turbulence simulation, in *Annual Research Briefs* (Center for Turbulence Research, Stanford University, 2015), pp. 43–54.
[28] M. R. Maxey and J. J. Riley, Equation of motion for a small rigid sphere in a uniform flow, Phys. Fluids **26**, 883 (1983).
[29] R. Gatignol, The Faxén formulas for a rigid particle in an unsteady non-uniform Stokes flow, J. Mech. Theor. Appl. **2**, 143 (1983).
[30] J. A. K. Horwitz, M. Rahmani, G. Geraci, A. J. Banko, and A. Mani, Two-way coupling effects in particle-laden turbulence: How particle-tracking scheme affects particle and fluid statistics, in *9th International Conference on Multiphase Flow, Firenze, Italy* (2016).
[31] D. Li, K. Luo, and J. Fan Z. Wang, W. Xiao, Drag enhancement and turbulence attenuation by small solid particles in an unstably stratified turbulent boundary layer, Phys. Fluids **31**, 063303 (2019).
[32] A. D. Bragg M. Carbone and M. Iovieno, Multiscale fluid-particle thermal interaction in isotropic turbulence, J. Fluid Mech. **881**, 679 (2019).

[33] P. Pakseresht and S. V. Apte, Volumetric displacement effects in Euler-Lagrange LES of particle-laden jet flows, Int. J. Multiphase Flow **113**, 16 (2019).
[34] K. Luo, Q. Dai, X. Liu, and J. Fan, Effects of wall roughness on particle dynamics in a spatially developing turbulent boundary layer, Int. J. Multiphase Flow **111**, 140 (2019).
[35] G. Wang, K. O. Fong, F. Coletti, J. Capecelatro, and D. H. Richter, Inertial particle velocity and distribution in vertical turbulent channel flow: A numerical and experimental comparison, Int. J. Multiphase Flow **120**, 103105 (2019).
[36] J. C. K. Tang, H. Wang, M. Bolla, A. Wehrfritz, and E. R. Hawkes, A DNS evaluation of mixing and evaporation models for TPDF modelling of nonpremixed spray flames, Proc. Combustion Inst. **37**, 3363 (2019).
[37] G. Wang and D. H. Richter, Modulation of the turbulence regeneration cycle by inertial particles in planar Couette flow, J. Fluid Mech. **861**, 901 (2019).
[38] S. Elghobashi and G. C. Truesdell, On the two-way interaction between homogeneous turbulence and dispersed solid particles. I: Turbulence modification, Phys. Fluids A **5**, (1993).
[39] S. Sundaram and L. R. Collins, A numerical study of the modulation of isotropic turbulence by suspended particles, J. Fluid Mech. **379**, 105 (1999).
[40] S. B. Pope, *Turbulent Flows* (Cambridge University Press, Cambridge, 2000).
[41] R. S. Rogallo, Numerical experiments in homogeneous turbulence, NASA Technical Memorandum B1315 (1981).
[42] S. Elghobashi, On predicting particle-laden turbulent flows, Appl. Sci. Res. **52**, 309 (1994).
[43] J. A. K. Horwitz, Verifiable point-particle methods for two-way coupled particle-laden flows, Ph.D. thesis, Stanford University, 2018.
[44] D. A. Donzis, P. K. Yeung, and K. R. Sreenivasan, Dissipation and enstrophy in isotropic turbulence: Resolution effects and scaling in direct numerical simulations, Phys. Fluids **20**, (2008).
[45] J. Bec, L. Biferale, A. Celani G. Boffetta, S. Musacchio M. Cencini, A. Lanotte, and F. Toschi, Acceleration statistics of heavy particles in turbulence, J. Fluid Mech. **550**, 349 (2006).
[46] G. K. Batchelor and A. A. Townsend, Decay of vorticity in isotropic turbulence, Proc. R. Soc. A **190**, 534 (1947).
[47] P. A. Davidson, *Turbulence: An Introduction for Scientists and Engineers* (Oxford University Press, 2004).
[48] C. W. Van Atta and R. A. Antonia, Reynolds number dependence of skewness and flatness factors of turbulent velocity derivatives, Phys. Fluids **23**, 252 (1980).
[49] G. Akiki, T. L. Jackson, and S. Balachandar, Pairwise interaction extended point-particle model for a random array of monodisperse spheres, J. Fluid Mech. **813**, 882 (2017).
[50] J. Horwitz and A. Mani, Simulations of decaying turbulence laden with particles: How are statistics affected by two-way coupling numerical scheme? in *68th Annual Meeting of the APS Division of Fluid Dynamics*, number 21, Boston, Massachusetts (American Physical Society, 2015).